NATIONAL ADVISORY COMMITTEE FOR AERONAUTICS

TECHNICAL NOTE

No. 984

STRESSES AT CUT-OUTS IN SHEAR RESISTANT WEBS AS DETERMINED BY THE PHOTOELASTIC METHOD

By Benjamin F. Ruffner and Calvin L. Schmidt
Oregon State College

Washington
October 1945

NATIONAL ADVISORY COMMITTEE FOR AERONAUTICS

TECHNICAL NOTE NO. 984

STRESSES AT CUT-OUTS IN SHEAR RESISTANT WEBS AS DETERMINED BY THE PHOTOELASTIC METHOD

By Benjamin F. Ruffner and Calvin L. Schmidt

SUMMARY

Stress concentration factors for shear stresses around cut-outs in the webs of beams having shear resistant webs were determined by the photoelastic method. Webs with circular, square, and rectangular cut-outs were tested. The effect of reinforcements around square and circular cut-outs was investigated. Results indicate that square and rectangular cut-outs having two sides parallel to the neutral axis of the beam should be avoided whenever possible. Circular cut-outs and square cut-outs, with sides at 45° to the neutral axis, produced lower stress concentration factors than the other two types.

INTRODUCTION

Cut-outs in shear webs occur frequently in aircraft structures. These are often desirable as lightening holes in web areas not highly stressed. In other regions cut-outs are necessary for installation of equipment. The purpose of this investigation was to determine the most efficient shape of cut-out and to determine the maximum stress concentration factors induced by various cut-outs. The photoelastic method was used for the investigation because the region of maximum stress and the amount of maximum stress is readily determinable by this method. Values for stress concentration factors determined by this method are, however, applicable only in the elastic range.

This investigation, conducted at Oregon State College, was sponsored by and conducted with the financial assistance of the National Advisory Committee for Aeronautics.

SYMBOLS

a	length of rectangular cut-out, inches (See fig. 14.)
b	height of rectangular cut-out, inches (See fig. 14.)
d_i	inner diameter of circular cut-out, inner width of square cut-out, inches (See figs. 7, 12, 13, 15.)
d_{ie}	effective diameter of cut-out, that is, diameter of circular hole of same area as cut-out under consideration, inches
d_o	outer diameter of circular reinforcement, outer width of square reinforcement, inches (See figs. 16, 17.)
h_1	width of metal flange on beam models, inches (See fig. 11.)
h_2	height of Bakelite web, inches (See fig. 11.)
k	distance between pins supporting shear-web models, inches
l	span of beams, inches
n	fringe order
r_c	inner radius of corners on square and rectangular cut-outs, inches (See figs. 13, 14, 15, 17.)
r_{co}	outer radius of reinforcement of square holes, inches (See fig. 17.)
t_B	thickness of Bakelite web, nonreinforced models, inches (See fig. 6.)
t_{B_1}	thickness of Bakelite webs, nonreinforced areas, inches (See fig. 7.)
t_{B_2}	thickness of reinforced section of Bakelite web, inches (See fig. 7.)
y	distance from neutral axis of beam, inches (See fig. 11.)
C	stress-optic coefficient, Brewsters
E	modulus of elasticity, pounds per square inch
F	stress concentration factor

I moment of inertia of beam, inches^4

K_1, K_2 constants

M bending moment, inch-pounds

R radius of curvature (fig. 11)

P load, pounds

W load, pounds

α ratio r_c/h_2

β ratio d_{ie}/h_2

τ shear stress, pounds per square inch

σ normal stress, pounds per square inch

σ_1, σ_2 principal stresses, pounds per square inch

ϵ unit tensile strain, pounds per square inch

λ wavelength of monochromatic light used in polariscope, angstrom units

Subscripts

B Bakelite

M metal

MODELS - TEST METHODS

General

Beam models were constructed with webs of Bakelite BT 61-893 and with flanges of brass. The construction of the models is described in subsequent paragraphs. The methods used for forming and finishing the Bakelite are described in detail in reference 1.

In order to obtain physical properties of the materials, needed in the analysis of beam results, models 1, 2, and 5

were used. The flanges of all models were identical and were cut from the same brass sheet used for the tension test specimen, model 1. For the Bakelite webs two different sheets of Bakelite stock were used. A calibration specimen was cut from each sheet.

Determination of Physical Properties of Materials

In figure 1 is shown the tension test specimen used for determination of the modulus of elasticity of brass. Strain measurements were obtained by use of Huggenberger tensometers. Results of this test are given in table I and figure 2. The modulus of elasticity of the brass was found to be 16.55×10^6 psi. Model 2 (shown in fig. 1) was used for the tension test of the Bakelite. Results of this test are shown in table II and figure 3. The modulus of elasticity of the Bakelite was 6.72×10^5 psi.

If σ_1 and σ_2 are the principal stresses at any point in a photoelastic model, the fringe order n, at this point, is proportional to $\sigma_1 - \sigma_2$. The constant of proportionality is a function of the thickness of the specimen in the direction of the light rays, the wavelength of the light used, and the stress-optic coefficient.

The stress-optic coefficient C is defined by:

$$C = \frac{n\lambda}{1.752\ t(\sigma_1 - \sigma_2)} \qquad (1)$$

For a particular model, using a fixed wavelength of light, write:

$$\sigma_1 - \sigma_2 = Kn \qquad (2)$$

The stress-optic coefficient C shows some variation in different sheets of the material. For this reason, tests to determine C were made on models 2 and 5. Drawings of these models are shown on figure 1. These were tested as simple beams loaded as shown in figures 4 and 5. At section A-A of these beams the only stresses present are normal stresses parallel to the sides of the beam. The shear is zero and no stress perpendicular to the beam axis is present. Therefore, there is obtained from equation (1), since $\sigma_2 = 0$,

$$\sigma_1 = -\frac{My}{I} = \frac{-n\lambda}{1.752\ (t_B)(C)}$$

or

$$C = \frac{-n\lambda\ I}{1.752\ (t_B)(y)\ M} \qquad (3)$$

The bending moment M was determined from the conditions of loading. The moment of inertia I was calculated from the model dimensions. The wavelength of light λ used in these tests was 5461 angstrom units. The fringe order n was plotted against distance y from the neutral axis. Values of y were measured from fringe photographs. Fringe patterns for these tests are shown on photographs 6 and 74. (See fig. 18.) The data obtained from these photographs are shown in tables III and IV and plotted on figures 4 and 5. Since the ratio n/y was a constant, the value of C may be found from equation (3). The stress-optic coefficient for model 2 was 35.8 Brewsters. This value was used on models 3, 4, 9, 10, and 11, which were all cut from the same sheet. The stress-optic coefficient for model 5 was 33.9 Brewsters. This value was used in calculations of results obtained from models 6 and 7, cut from the other sheet stock.

Description of Beam Models

Beam models were constructed with Bakelite webs. The same brass flanges were used for all models. In figure 6 is shown a drawing applicable to all models with nonreinforced cut-outs. Sizes and shapes of cut-outs are described in detail in tables and curves giving results of tests. The models of reinforced cut-outs were formed by cutting down the thickness of the Bakelite sheet except in the areas used to represent reinforcements. Drawings of reinforced cut-out models are shown in figures 7 and 8.

Each web model was tested with a number of different cut-out sizes and shapes. The cut-outs may, however, be separated into six different types:

1. Nonreinforced circular cut-outs

2. Nonreinforced square cut-outs with varying fillet radii in the corners and with various widths of squares. In this series two sides of the squares were parallel to the neutral axis of the beam.

3. Nonreinforced rectangular cut-outs with varying fillet radii, varying ratios of width to height of rectangle, and varying ratios of height of rectangle to depth of beam. Two sides of the rectangle were parallel to the neutral axis of the beam.

4. Nonreinforced square cut-outs with varying fillet radii and varying ratios of width of squares to depth of beam. The sides of the square were set at 45° to the neutral axis of the beam.

5. Reinforced circular cut-outs with constant outer diameter of reinforcement of 0.47 times the depth of the beam. The inner diameter of the cut-outs was varied from 0.167 to 0.375 times the depth of the beam.

6. Reinforced square cut-outs with constant inner dimensions. The outer width of the reinforcement dimension was varied from 0.243 to 0.916 times the beam depth. The sides of the square were at 45° to the neutral axis of the beam.

Method of Loading Models

Figure 9 shows a photograph of a model set up for test. Figure 10 is a sketch showing the geometry of the loading system. The models were tested as cantilever beams with half the load at the right end applied on the upper flange. In order to split the vertical reaction on the left end into two equal components, the model was held by a pin through the lower flange and loading frame. The upper support on the left end was a tension member. The angle θ at which this member was set to the horizontal was adjusted so that the vertical component of tension in the member was equal to $P/2$. This condition was obtained (see fig. 10) by making $\tan \theta = k/2l$. It is believed that this arrangement of the supports gives a more symmetrical distribution of shear stress in the webs than if no attempt were made to distribute the loads and reactions equally between the upper and lower flanges.

On all tests, the polariscope in the photoelastic laboratory at Oregon State College was used. The light source consisted of a mercury vapor lamp. Light filters were used so that a monochromatic light of wavelength 5461 angstrom units illuminated the field. Fringe patterns for all tests were recorded by means of photographs. Photographs were numbered in the order in which they were taken. A few typical fringe photographs used in this report are shown in

figure 19. The numbering system used on these includes four numbers. The first is the photograph number, the second is the model number, the third is the test number, and the fourth is the load in pounds. For instance, a photograph numbered 118-9-6-400 indicates photograph 118, model 9, test series 6, and load of 400 pounds. A few photographs numbers are omitted from the report for various reasons. When several exposures of the same test condition were made, only the clearest of these was included. Several times, photographs were taken with the polariscope adjusted for plane polarized light. All fringe photographs included in this report were taken with circularly polarized light, with quarter-wave plates crossed, unless otherwise noted. Some photographs were taken with the quarter-wave plates set parallel.

RESULTS AND ANALYSIS OF TESTS

Distribution of Shear Stress in Uncut Webs

In beams having relatively stiff flanges and thin webs, it may be assumed that the shear stress in the web is constant from the top to the bottom flange of the beam. In cases, however, where the bending stiffness of the web is appreciable, the shear stress varies with distance from the neutral axis. In the models tested some variation of shear stress occurs on the Bakelite web. This shear stress could have been obtained photoelastically, but, for purposes of definition of the stress concentration factor, the maximum shear stress in the uncut web was determined by calculation. Of interest in this report is the maximum shear stress at the neutral axis in the uncut web. This was used as a basis for the computation of the stress concentration factors. When the flanges and the web are constructed of materials of different elastic properties, the formula for maximum shear stress is complicated somewhat. If figure 11 is referred to for the notation, the equation for stresses in the beam models may be written as:

$$\sigma_B = \frac{-MyE_B}{(EI)_{eff}} \tag{4}$$

$$\sigma_M = \frac{-MyE_M}{(EI)_{eff}} \tag{5}$$

where

$$(EI)_{eff} = E_B I_B + E_M I_M \tag{6}$$

I_B moment of inertia of Bakelite web about beam neutral axis

I_M moment of inertia of metal flanges about beam neutral axis

Equation (5) is, of course, valid only for values of y from $\left(\frac{h_2}{2} - h_1\right)$ to $\frac{h_2}{2}$ and from $-\left(\frac{h_2}{2} - h_1\right)$ to $-\frac{h_2}{2}$.

The shear stress τ_{max} in the Bakelite web, at the neutral axis is given by

$$\tau_{max} = \frac{P}{t_B(EI)_{eff}}\left[E_B t_B \frac{h_2^2}{8} + 2E_M t_M h_1\left(\frac{h_2}{2} - \frac{h_1}{2}\right)\right] \tag{7}$$

For any particular model, equation (7) may be put in the form:

$$\tau_{max} = K_1 P \tag{8}$$

In table V are shown computations of K_1 for the various models tested. It should be noted that equations (4) to (8) are applicable only to beams constructed with a web of rectangular cross section, having two rectangular members acting as flanges at the top and bottom of the beam.

Determination of Stress Concentration Factor F

The stress concentration factor F is defined as the ratio of the maximum shear stress, at any point in the web of a model, to the computed maximum shear stress at the neutral axis for the same model with no cutout. The maximum shear stress at any point in a plane stressed body is given by $\tau = \frac{\sigma_1 - \sigma_2}{2}$. Therefore, from equation (2):

$$\tau = \frac{K}{2} n = K_2 n \tag{9}$$

The constant K_2 is, from equations (1) and (2),

$$K_2 = \frac{\lambda}{1.752(2)(t_B)\ C}$$

Since the wavelength of light λ was equal to 5461 angstrom units in all tests, this may be written:

$$K_2 = \frac{5461}{1.752(2)} \frac{1}{t_B C} = \frac{1559}{t_B C} \tag{10}$$

In table VI are values of K_2 computed for the various models.

The maximum shear stress, in the models with cut-outs, occurred at some point on the boundary of the cut-outs. On each fringe photograph is marked the point of maximum shear stress and the fringe order at this point.

The stress concentration factor may then be written:

$$F = \frac{K_2 n}{K_1 P} \tag{11}$$

when n is the maximum fringe order on the photograph for the test of the cut-out model.

Equations (8), (9), and (11) are applicable in the region where Hooke's law applies. If the stress in the Bakelite exceeds the elastic limit these are no longer valid. In all tests, however, the maximum fringe order n gave stresses below the elastic limit of the material used.

Definition of Effective Diameter of Cut-Outs

In order to compare the stress concentration factors for the various cut-outs, the effective diameter d_{ie} is

introduced. This is the diameter of a circular cut-out of the same area as the cut-out under consideration. For rectangular cut-outs, this is:

$$d_{ie} = \sqrt{\frac{4A}{\pi}} = 1.128\sqrt{A} = 1.128\sqrt{ab - 0.8584\ r_c^2} \qquad (12)$$

For square holes $ab = d_i^2$; so equation (12) becomes:

$$d_{ie} = 1.128\sqrt{d_i^2 - 0.8584\ r_c^2} \qquad (13)$$

For circular holes $d_{ie} = d_i$.

Wherever possible, results of tests were plotted in nondimensional form. The factor F is nondimensional. Dimensions of cut-outs were divided by the height of the web h_2 to put these in nondimensional form. The ratio d_{ie}/h_2 is denoted by β.

Tests of Nonreinforced Circular Cut-Outs

A large number of tests of circular cut-outs were made. These were used to establish the curve of stress concentration factor against ratio of diameter to depth of web. The plot of these in figure 12 also gives an indication of the accuracy of the test methods if the dispersion of the points is considered. The fringe order n was obtained for each test by ccunting the fringes as they appeared during loading. In some cases fringes are so close together near the region of maximum fringe order that examination of the fringe photographs under a microscope was necessary to determine n. In general, the results are accurate to within plus or minus one fringe order. In a few cases, owing to residual optical effects on the edge of the cut-outs, the value of n may be in error as much as two fringes. However, if the model shows no "edge effects" (reference 3) in the unloaded condition, the value of n may be determined to a fraction of a fringe order. It is believed that this curve as drawn in figure 12 represents the stress concentration factors within an error of 3 percent at any point.

In table VII and figure 12 are given the results of the nonreinforced circular cut-out tests. Timoshenko (reference

2) gives the theoretical solution for the stress concentration factor for a circular hole in an infinite plate under uniform shear. This indicates that $F = 2.0$ at the point of maximum stress. The curve of figure 12 shows that as the diameter of the circular cut-out approaches zero the stress concentration factor approaches the theoretical value.

At the smaller values of β it is believed that results shown on figure 12 are quite accurate. At higher β values the results may be influenced to some extent by the size and shape of the flange members. However, for these large cut-outs, the factors as given should be safe for use in design.

The region of highest stress, at the circular cut-out boundaries, occurred in all tests at points approximately 45° from the neutral axis of the beam. If stresses due only to shear and none due to bending were present, the fringe patterns would be symmetrical about the vertical axis through the center of the circular cut-out. Owing, however, to the presence of some stress in the web due to bending, this was not the case. For this reason, stress concentration factors given here are probably slightly conservative for pure shear webs. Even for large cut-outs, however, such as shown on photograph 152, the fringe pattern is very nearly symmetrical. Therefore, the degree of error in the stress concentration factor from this cause should be small.

In order to investigate the effect, if any, of the depth-span ratio of the web, model 9 was constructed with a web deeper than that used on other models. The results of this test plot quite well on the faired curve. This indicates that the results obtained for stress concentration factors are dependent on β but not, at least in the regions tested, on the ratio of h_2 to the span of beam. It is believed that this is sufficient experimental verification to justify the use of the curve plotted in figure 12.

In order to obtain an empirical formula to represent the curve of figure 12, it was assumed that this could be represented by a cubic of the form:

$$F = a_0 + a_1\beta + a_2\beta^2 + a_3\beta^3 \qquad (14)$$

A least square analysis of the faired curve was used to determine the values of the constant, a_0, a_1, a_2, and a_3. The following empirical formula, thus determined:

$$F = 2.000 + 4.214\,\beta - 3.46\,\beta^2 + 12.5\,\beta^3 \qquad (15)$$

gives a good approximation to the faired curve in the region from $\beta = 0$ to $\beta = 0.7$.

Tests of Nonreinforced Square Cut-Outs with Sides of Squares Parallel to Neutral Axes of Beams

In these tests the stress was found to be highest at the corners of the squares. The stress concentration factor was determined to be a function of $\alpha = \frac{r_c}{h_2}$, as well as $\beta = \frac{d_{ie}}{h_2}$. A square hole with $\alpha = \frac{1}{2}\beta$ is identical to a circular hole of radius r_c. The results of this series of tests are given in table VIII and figure 13. Since the curves of figure 13 are plotted against $\beta = \frac{d_{ie}}{h_2}$, cut-outs of the same area are all found on the same vertical lines. The straight lines representing stress concentration factors for the square holes with constant values of α were first plotted for values of α as tested. It was then found that these straight lines would fair the data quite well if all were drawn from the same point $F = -8.84$ and $\beta = -0.594$. A series of straight lines for various values of α were then plotted. An empirical formula representing the slope of these lines was found by a least square analysis. This is:

$$\frac{dF}{d\beta} = 18.22 - 42.85\,\alpha + 81.6\,\alpha^2 \qquad (16)$$

When equation (16) was combined with equation (15), the following empirical equation for the stress concentration factor F as a function of α and β was obtained:

$$F = 2.000 - 28.012\,\alpha + 71.86\,\alpha^2 - 63.2\,\alpha^3 + (18.22 - 42.85\,\alpha + 81.6\,\alpha^2)\,\beta \qquad (17)$$

This formula is accurate in the region $\beta = 2\alpha$ to $\beta = 0.50$. It can be used with fair accuracy for values of β up to 0.600 but should not be trusted to give correct values of F for β greater than 0.6. This is an empirical formula based on experimental results in the region $\beta = 0$ to $\beta = 0.5$ and has no rational basis that justifies its use for the larger values of β. While equation (17) may give accurate values at higher values of β, no experimental evidence in this study is available to prove this.

The results of these tests indicate that, wherever possible, the use of square holes, with two sides parallel to the neutral axis of the beam, should be avoided.

Tests of Nonreinforced Rectangular Cut-Outs

The results of rectangular cut-out tests are given in table IX and figure 14. These indicate that, when the height of cut-out b is large, the stress concentration factor increases more rapidly with β than at the smaller values of b.

In figure 14 the slopes of these stress concentration curves are plotted against F for $\frac{a}{b} = 1.0$. An approximate expression for this is:

$$\frac{dF}{d\left(\frac{a}{b}\right)} = -1.26 + 0.79\, F_{(a/b)=1.0} \qquad (18)$$

The stress concentration factor is then:

$$F = 1.26 + 0.21\, F_{(a/b)=1} + \left(0.79\, F_{(a/b)=1} - 1.26\right)\frac{a}{b} \qquad (19)$$

where $F_{(a/b)=1.0}$ is the stress concentration factor for the square cut-out with $\frac{d_1}{h_2} = \frac{b}{h_2}$ and with α the same as for the rectangular cut-out. This empirical formula fits the test data with good accuracy. On figure 14 faired test curves and plots of equation (19) are shown for comparison.

In these tests stress concentration factors were high, indicating that rectangular cut-outs should be avoided

whenever possible. No tests were made with a/b ratios less than 1.0. It appears reasonable to expect, however, that the empirical formula (equation (19)) will be applicable at a/b ratios of somewhat less than 1.0.

Tests of Nonreinforced Square Cut-Outs with Sides of Squares at 45° to Beam Flanges

Since, in the circular cut-out tests, the maximum stress occurred at points 45° from the diameter parallel to the beam flanges, it appeared desirable to test cut-outs with the radius increased at these points. This was accomplished by making square cut-outs as illustrated on figure 15. The results of these tests are given in table X and figure 15. The corner radius ratio α was used as abscissa and values of β were used as parameters for plotting these results. It is interesting to note here that small radii in the corners are desirable for small ratios of β. The photographs of the fringe patterns for these tests show that the maximum stress does not occur at the corners but at points on the sides of the squares near the corners. An examination of these photographs also shows that areas of high stress are relatively small as compared to areas of high stress on circular cut-outs and square cut-outs having two sides parallel to beam neutral axis.

The curves of figure 15 are the result of cross plots. First, F was plotted against β for constant values of α and the experimental results faired. These curves were then replotted with β as parameter and α as abscissa. The experimental points, with corresponding photograph numbers, are marked on the curves for comparison with table X and fringe photographs.

Tests of Reinforced Circular Cut-Outs

Results of tests of reinforced cut-outs are shown in table XI and figure 16. In this series the reinforcement was also circular. The outer diameter of the reinforcement was kept constant at a d_o/h_2 ratio of 0.470. The inner diameter was varied from 0.167 to 0.375 h_2. The reinforcements, if fully effective, might be expected to reduce the stress concentration factor at the edge of the hole inversely as the ratio of the thickness of the reinforced area to the thickness of the nonreinforced web. This, however, is not

the case, as an examination of figure 16 will show. The maximum stress concentration factor in the reinforced sections averages approximately 20 percent higher than if the reinforcement were fully effective. It is of interest that a fairly narrow reinforcement appears to be as effective in the reinforced section as a fairly wide reinforcement. Since the maximum stress occurs on a relatively small area of the boundary of the cut-out, the reinforcement of this area appears to be the most important factor in reducing the maximum shear stress at the hole boundary. In practice, the purpose of this reinforcement would be to increase the stiffness around the cut-out as well as to decrease the stress concentration factor. Larger reinforcements might be advisable for that purpose. It is possible that the maximum stresses may be in the sheet at the boundary of the reinforcement rather than at the edge of the hole.

Tests of Reinforced Square Cut-Outs with Sides of Squares at 45° to Beam Neutral Axes

In this series the inner dimensions of the cut-out were kept constant and the outer dimensions of the reinforcement were reduced in increments. The results of these tests are given in table XII and figure 17.

In figure 15 the value of F for $\beta = 0.196$ and $\alpha = 0.031$ is 3.00. If the reinforcement were fully effective, the stress concentration factor for the reinforced cut-out would be:

$$\frac{t_{B_1}}{t_{B_2}} (3.00) = \frac{0.133}{0.310} (3.00) = 1.28$$

The curve of figure 17 approaches this value as d_o/h_2 approaches 1.0. On these models the reinforcements act as beams in bending. The beam action of the reinforcements is apparent upon examination of photographs 144, 149, and 150. These beams may be considered to transmit the principal stresses σ_1 and σ_2, in the webs, around the cut-out by shear force in the beams.

From figure 17 it appears that an economical reinforcement for such diagonal square holes would have a width equal to approximately half the width of the side of the square.

The thickness of this could be such that the maximum shear stress at the reinforced section is equal to or less than that in the uncut web.

CONCLUSIONS

The stress concentration factors determined from photoelastic test give a basis for design of lightening holes and cut-outs in shear-resistant webs. For webs in which allowable stresses are determined by critical buckling stresses, the stress concentration factors can be used as a guide. In that case, regions where buckling is liable to occur are indicated by high stress. These regions may then be stiffened to prevent this. The empirical formulas derived are suggested for design use in the range of parameters for which they were determined.

It is believed that the stress concentration factors obtained are accurate within 5 percent as long as the maximum stresses are within the elastic range. Where yield of the material in the region of high stress occurs, the stresses will probably be redistributed so that the stress concentration factors given here will be conservative. If buckling of the web in the region of the cut-outs occurs, a redistribution of stress also will occur. If this happens, however, the edges of the cut-out should be reinforced to prevent collapse of the web in this region.

The effect of web cut-outs on the effective stiffness of the beam as a whole cannot be determined photoelastically. However, from a study of the fringe photographs, the extent of highly stressed areas may be observed. If a large area around the cut-out is highly stressed, the deformation of the web will be higher than if only small areas around the cut-outs are highly stressed. By this reasoning, the following tentative conclusions as to the effect of web cut-outs on the stiffness of the beam may be drawn:

1. Square and rectangular cut-outs, having two sides parallel to the neutral axis, not only showed high stress concentrations at the corners, but large areas in the vicinity of the cut-outs were also highly stressed. It appears from this that the stiffness of the beam as a whole would be considerably diminished if such cut-outs were used.

2. Circular cut-outs, and square cut-outs with sides of squares at 45° to the neutral axis, not only showed lower

stress concentration factors at the edges of the cut-out, but the areas of high stress were considerably smaller. This indicates that the reduction in beam stiffness was less than for the other types.

The stress concentration factors were based on values of maximum shear stress in the uncut web, calculated according to conventional methods. The results of tests should be applied as follows:

1. The shear stress in the uncut web should be computed by conventional methods.

2. By use of the empirical formulas or curves given in this report, the stress concentration factor F should be determined.

3. The maximum shear stress may then be obtained by multiplying F by the calculated value of shear stress obtained for the uncut web.

If reinforcements are used only to reduce the value of the maximum stress at the edge of the cut-out, the results indicate that the consideration of the following will lead to more efficient use of material:

1. The width, in the plane of the web, of the reinforcement need not be greater than approximately half the width of the cut-out. Wider reinforcements do not cause appreciable reductions in the stress concentration at the edge of the cut-out.

2. A thickness of reinforcing sheet about 20 percent greater than the stress concentration factor times the web thickness will reduce the maximum stress to a value approaching that in the uncut web.

If the reinforcing material is used to restore stiffness to the beam as well as to reduce the local stresses, the thickness of the reinforcing material will probably be determined from consideration of stress concentration; whereas the width of reinforcing material may be determined by considerations of stiffness.

Oregon State College,
Corvallis, Oregon, August 27, 1944.

REFERENCES

1. Ruffner, Benjamin F., Jr.: Stress Analysis of Fuselage Bulkheads by the Photoelastic Method. NACA TN No. 870, 1942.

2. Timoshenko, S.: Theory of Elasticity. McGraw-Hill Book Co., Inc., 1934.

3. Frocht, Max Mark: Photoelasticity. Vol. I. John Wiley & Sons, Inc., 1941.

TABLE I

DATA FROM TENSION TEST OF MODEL NO. 1.
(Brass)

Tensile Stress σ	Tensile Strain ϵ
794	0.000032
1585	.000076
2380	.000122
3170	.000168
3965	.000211
4755	.000261
5550	.000312
6345	.000362
7140	.000412
7930	.000498

TABLE II

DATA FROM TENSION TEST OF MODEL NO. 2.
(Bakelite BT 61-893)

Tensile Stress σ	Tensile Strain ϵ
73	0.000103
146	.000198
219	.000298
292	.000404
365	.000516
438	.000618
511	.000723
584	.000840
657	.000942
438	.000617
292	.000396
146	.000177

TABLE III

DATA FROM CALIBRATION TEST OF MODEL NO. 2.

Fringe Order n	Distance from Zero Fringe
- 9.9 (Top edge)	0.253
- 9.0	.231
- 8.0	.203
- 7.0	.176
- 6.0	.151
- 5.0	.125
- 4.0	.099
- 3.0	.075
- 2.0	.049
- 1.0	.024
0.0	.000
1.0	- .025
2.0	- .050
3.0	- .075
4.0	- .100
5.0	- .123
6.0	- .147
7.0	- .171
8.0	- .195
9.0	- .219
10.0	- .242
10.2 (Bottom edge)	- .254

TABLE IV

DATA FROM CALIBRATION TEST OF MODEL NO. 5.

Fringe Order n	Distance from Zero Fringe
-10.0 (Top edge)	0.243
- 9.0	.218
- 8.0	.197
- 7.0	.166
- 6.0	.145
- 5.0	.119
- 4.0	.095
- 3.0	.073
- 2.0	.047
- 1.0	.024
0.0	.000
1.0	- .023
2.0	- .047
3.0	- .067
4.0	- .093
5.0	- .116
6.0	- .140
7.0	- .161
8.0	- .183
9.0	- .207
10.0	- .232
10.5 (Bottom edge)	- .245

TABLE V

COMPUTATIONS OF K_1

$E_M = 16.55 \times 10^6$, $t_M = 0.1235"$, $b = 0.50"$, $E_B = 672{,}000$

1	2	3	4	5	6	7	8	9	10	11	12	13	14	15
Model No.	t_B	h_2	I_B	I_M	$E_B I_B$ $\times 10^{-6}$	$E_M I_M$ $\times 10^{-6}$	$(EI)_{eff}$ $\times 10^{-6}$	$E_B t_B \frac{h_2^2}{8}$ $\times 10^{-6}$	$2E_M t_M b$ $\times 10^{-6}$	$\frac{h}{2} - \frac{h_1}{2}$	(10)X(11) $\times 10^{-6}$	[(9)+(12)] $\times 10^{-6}$	$t_B EI_{eff}$ $\times 10^{-6}$	K_1
3	0.269	2.99	0.598	0.388	0.402	6.42	6.82	0.202	2.042	1.245	2.55	2.752	1.835	1.498
4	.275	2.97	.598	.383	.402	6.34	6.74	.204	2.042	1.235	2.53	2.734	1.855	1.475
6	.283	3.00	.637	.390	.428	6.46	6.89	.214	2.042	1.250	2.56	2.774	1.950	1.423
7	.274	3.01	.624	.392	.419	6.48	6.90	.208	2.042	1.255	2.57	2.778	1.900	1.455
9	.265	5.48	3.640	1.536	2.442	25.42	27.86	.670	2.042	2.490	5.10	5.770	7.370	.782
10	.120	3.01	.278	.392	.187	6.48	6.67	.091	2.042	1.255	2.57	2.661	.798	3.320
11	.133	3.00	.300	.390	.201	6.46	6.66	.101	2.042	1.250	2.56	2.661	.885	3.000

TABLE VI

COMPUTATIONS OF K_2

Model No.	t_B	C	$t_B \cdot C$	K_2
3	0.269	35.8	9.64	161.5
4	.275	35.8	9.85	158.2
6	.283	33.9	9.60	163.0
7	.274	33.9	9.26	168.0
9	.265	35.8	9.48	165.0
10	.259	35.8	9.27	168.0
11	.310	35.8	11.09	140.3

TABLE VII

RESULTS OF TESTS FOR F ON NONREINFORCED CIRCULAR CUT-OUTS

Photo No.	Model No.	Test No.	Load P	h_2	t_B	$d_1 = d_{1e}$	$\frac{d_{1e}}{h_2} \cdot \beta$	K_2	n	τ_{max}	K_1	$K_1 P$	F
9	3	1	250	2.99	0.269	0.125	0.042	161.5	5.0	807	1.498	374	2.16
12	3	1	125	2.99	.269	.250	.084	161.5	3.0	484	1.498	187	2.58
13	3	1	260	2.99	.269	.250	.084	161.5	5.2	840	1.498	389	2.16
17	3	1	250	2.99	.269	.406	.136	161.5	6.7	1082	1.498	374	2.89
20	3	1	150	2.99	.269	.500	.167	161.5	4.2	678	1.498	225	3.01
21	3	1	250	2.99	.269	.500	.167	161.5	6.5	1050	1.498	374	2.81
25	3	1	250	2.99	.269	.600	.200	161.5	7.1	1145	1.498	374	3.06
26	3	1	250	2.99	.269	.600	.200	161.5	7.1	1145	1.498	374	3.06
28	3	1	150	2.99	.269	.875	.293	161.5	4.8	775	1.498	225	3.45
29	3	1	260	2.99	.269	.875	.293	161.5	8.0	1291	1.498	389	3.32
30	3	1	260	2.99	.269	.875	.293	161.5	8.0	1291	1.498	389	3.32
33	3	1	250	2.99	.269	1.000	.334	161.5	8.3	1340	1.498	374	3.59
34	3	1	250	2.99	.269	1.000	.334	161.5	8.3	1340	1.498	374	3.59
37	3	1	250	2.99	.269	1.125	.376	161.5	8.7	1403	1.498	374	3.76
38	3	1	250	2.99	.269	1.125	.376	161.5	8.7	1403	1.498	374	3.76
40	3	1	150	2.99	.269	1.250	.418	161.5	5.8	946	1.498	225	4.21
41	3	1	250	2.99	.269	1.250	.418	161.5	9.0	1452	1.498	374	3.89
42	3	1	250	2.99	.269	1.250	.418	161.5	9.0	1452	1.498	374	3.89
43	3	1	325	2.99	.269	1.250	.418	161.5	11.5	1858	1.498	487	3.81
44	3	1	400	2.99	.269	1.250	.418	161.5	14.1	2278	1.498	598	3.81
81	6	3	300	3.00	0.283	0.250	0.083	163	6.0	976	1.423	427	2.29
83	6	3	300	3.00	.283	.500	.167	163	8.2	1335	1.423	427	3.13
86	6	3	300	3.00	.283	.750	.250	163	9.8	1598	1.423	427	3.74
91	6	3	300	3.00	.283	1.060	.354	163	11.0	1792	1.423	427	4.20
98	7	4	300	3.01	.274	.250	.083	168	6.5	1092	1.455	437	2.50
100	7	4	300	3.01	.274	.500	.166	168	7.0	1175	1.455	437	2.69
103	7	4	300	3.01	.274	.750	.249	168	9.9	1662	1.455	437	3.81
107	7	4	300	3.01	.274	1.070	.356	168	10.5	1765	1.455	437	4.00
116	9	6	400	5.48	.265	.250	.046	165	3.6	593	.780	312	1.90
117	9	6	400	5.48	.265	.530	.097	165	4.8	792	.780	312	2.54
118	9	6	400	5.48	.265	.790	.144	165	5.7	941	.780	312	3.02
119	9	6	400	5.48	.265	1.101	.201	165	5.2	858	.780	312	2.75
120	9	6	400	5.48	.265	1.250	.228	165	5.3	875	.780	312	2.80
121	9	6	400	5.48	.265	1.500	.274	165	6.0	990	.780	312	3.17
122	9	6	400	5.48	.265	1.750	.319	165	6.6	1088	.780	312	3.48
123	9	6	400	5.48	.265	2.000	.365	165	6.7	1105	.780	312	3.55
124	9	6	400	5.48	.265	2.270	.414	165	7.5	1238	.780	312	3.96
125	9	6	400	5.48	.265	2.510	.458	165	8.0	1319	.780	312	4.22
148	9	6	400	5.48	.265	3.000	.547	165	10.0	1650	.780	312	5.28
151	9	6	400	5.48	.265	3.820	.697	165	14.5	2390	.780	312	7.67
152	9	6	400	5.48	.265	4.030	.735	165	16.5	2720	.780	312	8.72
153	7	4	300	3.01	.274	1.520	.505	168	12.5	2100	1.455	437	4.79
154	7	4	300	3.01	.274	1.760	.585	168	13.7	2300	1.455	437	5.22

TABLE VIII

RESULTS OF TESTS FOR F ON NONREINFORCED SQUARE CUT-OUTS
SIDES OF CUT-OUTS PARALLEL TO BEAM FLANGES

Photo No.	Model No.	Test No.	Load P	h_2	t_B	d_1	r_c	d_{1e}	$\frac{d_{1e}}{h_2}=\beta$	$\frac{r_c}{h_2}=\alpha$	K_2	n	τ_{max}	K_1	K_1P	F
46	4	2	300	2.97	0.275	0.328	0.000	0.370	0.125	0.000	158	12.0	1890	1.475	443	4.26
55	4	2	300	2.97	.275	.520	.125	.574	.193	.042	158	12.0	1890	1.475	443	4.23
59	4	2	300	2.97	.275	.780	.250	.840	.282	.084	158	11.7	1850	1.475	443	4.17
60	4	2	300	2.97	.275	.780	.250	.840	.282	.084	158	11.6	1830	1.475	443	4.12
61	4	2	300	2.97	.275	.790	.125	.879	.295	.042	158	16.5	2610	1.475	443	5.88
62	4	2	300	2.97	.275	.790	.125	.879	.295	.042	158	16.5	2610	1.475	443	5.88
63	4	2	300	2.97	.275	.790	.063	.887	.299	.021	158	18.0	2840	1.475	443	6.42
64	4	2	300	2.97	.275	.790	.063	.887	.299	.021	158	18.0	2840	1.475	443	6.42
82	6	3	300	3.00	.283	.250	.063	.276	.092	.021	163	8.3	1352	1.423	427	3.16
84	6	3	300	3.00	.283	.500	.125	.550	.183	.042	163	11.0	1790	1.423	427	4.19
85	6	3	300	3.00	.283	.500	.063	.561	.187	.021	163	12.3	2005	1.423	427	4.71
87	6	3	300	3.00	.283	.750	.250	.802	.267	.083	163	12.0	1955	1.423	427	4.57
88	6	3	300	3.00	.283	.760	.125	.847	.282	.042	163	15.5	2530	1.423	427	5.92
89	6	3	300	3.00	.283	.765	.063	.858	.286	.021	163	17.0	2770	1.423	427	6.48
92	6	3	300	3.00	.283	1.060	.375	1.128	.376	.125	163	13.0	2120	1.423	427	4.96
93	6	3	300	3.00	.283	1.080	.250	1.189	.396	.083	163	15.5	2530	1.423	427	5.92
94	6	3	300	3.00	.283	1.090	.125	1.220	.406	.042	163	20.5	3340	1.423	427	7.82
95	6	3	200	3.00	.283	1.090	.063	1.228	.409	.021	163	15.5	2525	1.423	285	8.83
96	6	3	300	3.00	.283	1.090	.063	1.228	.409	.021	163	23.0	3750	1.423	427	8.78

TABLE IX

RESULTS OF TESTS FOR F ON NONREINFORCED RECTANGULAR CUT-OUTS.
SIDES OF CUT-OUTS PARALLEL TO BEAM FLANGES

Photo No.	Model No.	Test No.	Load P	h_2	t_B	a	b	r_c	d_{1e}	$\frac{d_{1e}}{h_2}=\beta$	$\frac{r_c}{h_2}=\alpha$	$\frac{a}{b}$	$\frac{b}{h_2}$	K_2	n	τ_{max}	K_1	K_1P	F
46	4	2	300	2.97	0.275	0.328	0.328	0.000	0.370	0.125	0.000	1.00	0.110	158	12.0	1890	1.475	443	4.26
51	4	2	300	2.97	.275	.388	.328	.000	.402	.135	.000	1.15	.110	158	13.0	2050	1.475	443	4.62
53	4	2	300	2.97	.275	.500	.328	.000	.456	.153	.000	1.52	.110	158	15.0	2370	1.475	443	5.35
55	4	2	300	2.97	.275	.520	.520	.125	.574	.193	.042	1.00	.175	158	12.0	1885	1.475	443	4.23
57	4	2	300	2.97	.275	.750	.540	.125	.705	.237	.042	1.39	.182	158	14.0	2210	1.475	443	4.98
61	4	2	300	2.97	.275	.790	.790	.125	.879	.295	.042	1.00	.266	158	16.5	2610	1.475	443	5.88
63	4	2	300	2.97	.275	.790	.790	.063	.887	.299	.021	1.00	.266	158	18.0	2840	1.475	443	6.42
65	4	2	300	2.97	.275	1.000	.820	.125	1.010	.340	.042	1.22	.276	158	18.0	2850	1.475	443	6.42
67	4	2	300	2.97	.275	1.000	.830	.063	1.025	.345	.021	1.21	.279	158	20.5	3240	1.475	443	7.30
69	4	2	300	2.97	.275	1.250	.870	.125	1.169	.393	.042	1.44	.293	158	20.0	3160	1.475	443	7.12
72	4	2	250	2.97	.275	1.270	.880	.063	1.190	.401	.021	1.44	.296	158	19.0	3000	1.475	369	8.14

TABLE X

RESULTS OF TESTS FOR F ON NONREINFORCED SQUARE CUT-OUTS. SIDES OF CUT-OUTS 45° TO BEAM FLANGES

Photo No.	Model No.	Test No.	Load P	h_2	t_B	d_i	r_c	d_{ie}	$\frac{d_{ie}}{h_2}=\beta$	$\frac{r_c}{h_2}=\alpha$	K_2	n	τ_{max}	K_1	K_1P	F
99	7	4	300	3.01	0.274	0.250	0.063	0.275	0.091	0.021	168	5.8	975	1.455	437	2.23
101	7	4	300	3.01	.274	.500	.125	.548	.182	.042	168	8.0	1345	1.455	437	3.08
102	7	4	300	3.01	.274	.500	.063	.560	.186	.021	168	7.5	1260	1.455	437	2.88
104	7	4	300	3.01	.274	.750	.250	.802	.267	.083	168	9.0	1512	1.455	437	3.47
105	7	4	300	3.01	.274	.760	.125	.847	.281	.042	168	9.5	1597	1.455	437	3.65
106	7	4	300	3.01	.274	.770	.063	.864	.287	.021	168	9.2	1545	1.455	437	3.54
108	7	4	300	3.01	.274	1.070	.375	1.138	.378	.125	168	10.7	1798	1.455	437	4.12
109	7	4	300	3.01	.274	1.080	.250	1.192	.396	.083	168	11.5	1932	1.455	437	4.43
110	7	4	300	3.01	.274	1.090	.125	1.222	.406	.042	168	12.0	2015	1.455	437	4.61
111	7	4	300	3.01	.274	1.090	.063	1.227	.407	.021	168	12.2	2050	1.455	437	4.69

TABLE XI

RESULTS OF TESTS FOR F ON REINFORCED CIRCULAR CUT-OUTS. $(\frac{d_o}{h_2} = 0.470)$

Photo No.	Model No.	Test No.	Load P	h_2	t_{B1}	t_{B2}	d_i	$\frac{d_i}{h_2}$	K_2	n	τ_{max}	K_1	K_1P	F
132	10	7	150	3.00	0.120	0.259	0.500	0.167	168	4.6	772	332	498	1.54
133	10	7	150	3.00	.120	.259	.625	.209	168	4.9	822	332	498	1.65
134	10	7	150	3.00	.120	.259	.750	.250	168	5.2	874	332	498	1.75
135	10	7	150	3.00	.120	.259	.875	.291	168	5.5	924	332	498	1.85
136	10	7	150	3.00	.120	.259	1.000	.333	168	5.7	957	332	498	1.92
137	10	7	150	3.00	.120	.259	1.125	.375	168	5.8	975	332	498	1.96

TABLE XII

RESULTS OF TESTS FOR F ON REINFORCED SQUARE CUT-OUTS.
SIDES OF CUT-OUTS 45° TO BEAM FLANGES

Photo No.	Model No.	Test No.	Load P	h_2	t_{B1}	t_{B2}	d_i	d_o	r_c	d_{ie}	$\frac{d_{ie}=\beta}{h_2}$	$\frac{r_{c=\alpha}}{h_2}$	$\frac{d_o}{h_2}$	K_2	n	τ_{max}	K_1	K_1P	F
138	11	8	175	3.00	0.133	0.310	0.53	2.75	0.94	0.587	0.196	0.094	0.916	140.2	4.8	672	3.00	525	1.280
140	11	8	175	3.00	.133	.310	.53	2.20	.94	.587	.196	.094	.734	140.2	4.8	672	3.00	525	1.280
141	11	8	175	3.00	.133	.310	.53	1.73	.94	.587	.196	.094	.576	140.2	5.1	715	3.00	525	1.360
142	11	8	175	3.00	.133	.310	.53	1.25	.94	.587	.196	.094	.417	140.2	5.3	743	3.00	525	1.418
143	11	8	175	3.00	.133	.310	.53	1.00	.94	.587	.196	.094	.333	140.2	5.6	785	3.00	525	1.495
144	11	8	175	3.00	.133	.310	.53	.73	.94	.587	.196	.094	.243	140.2	6.4	897	3.00	525	1.710
149	11	8	200	3.00	.133	.310	.53	.73	.94	.587	.196	.094	.243	140.2	7.5	1052	3.00	600	1.753
150	11	8	225	3.00	.133	.310	.53	.73	.94	.587	.196	.094	.243	140.2	8.5	1192	3.00	675	1.785

MODEL NO. 1
BRASS TENSION SPECIMEN

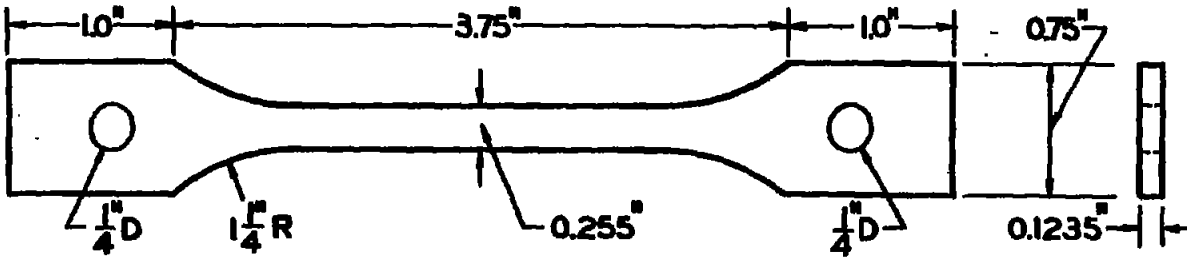

MODEL NO. 2
BAKELITE BT 61-893

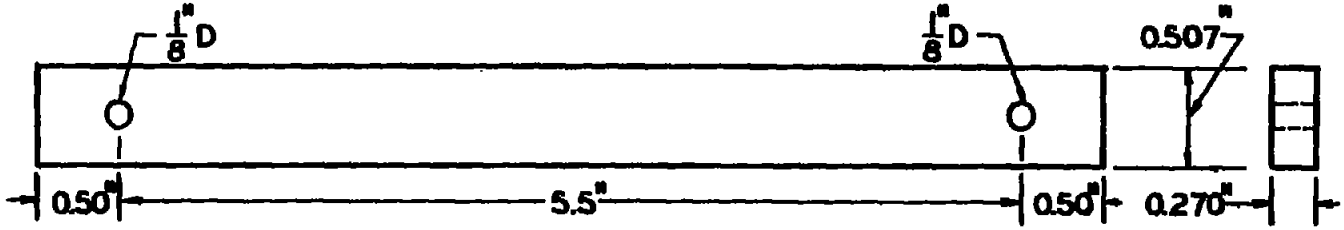

MODEL NO. 5
BAKELITE BT 61-893

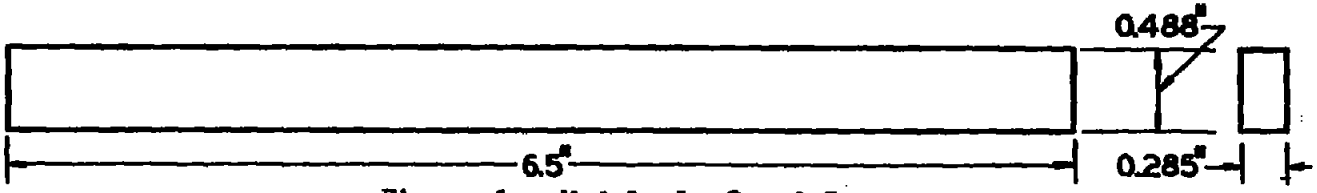

Figure 1.- Models 1, 2 and 5.

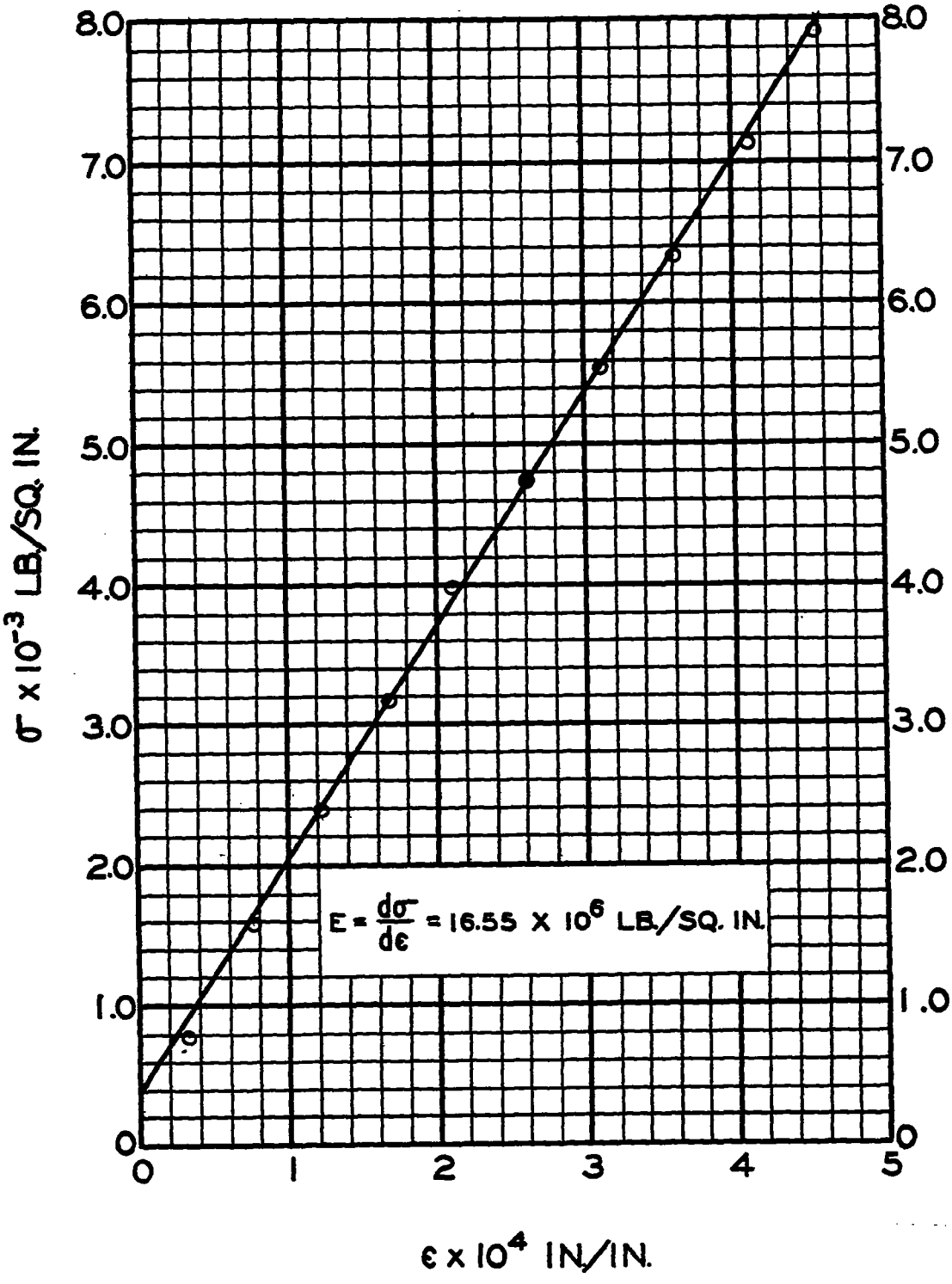

Figure 2.- Stress-strain curve of brass.

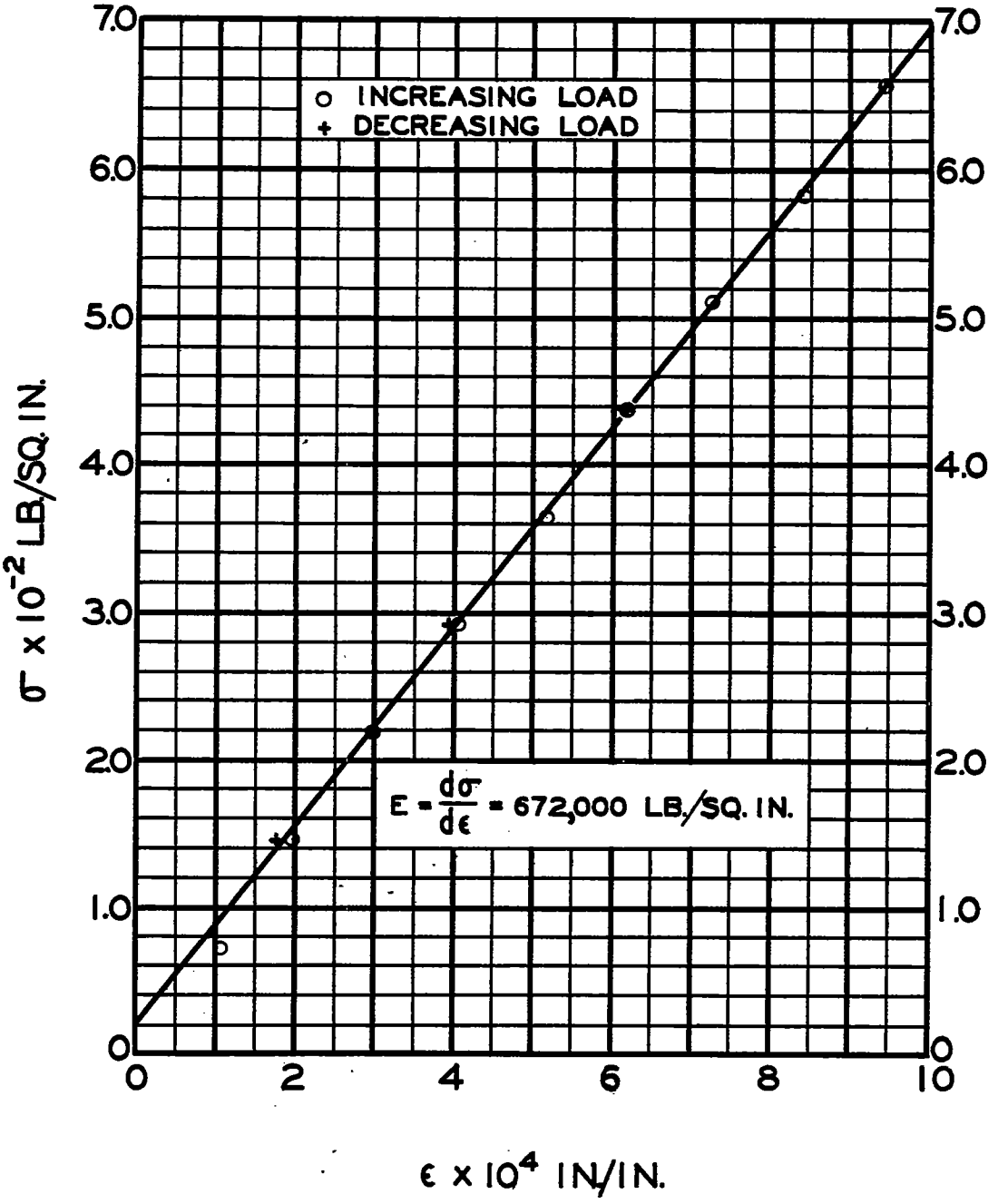

Figure 3.- Stress-strain of bakelite.

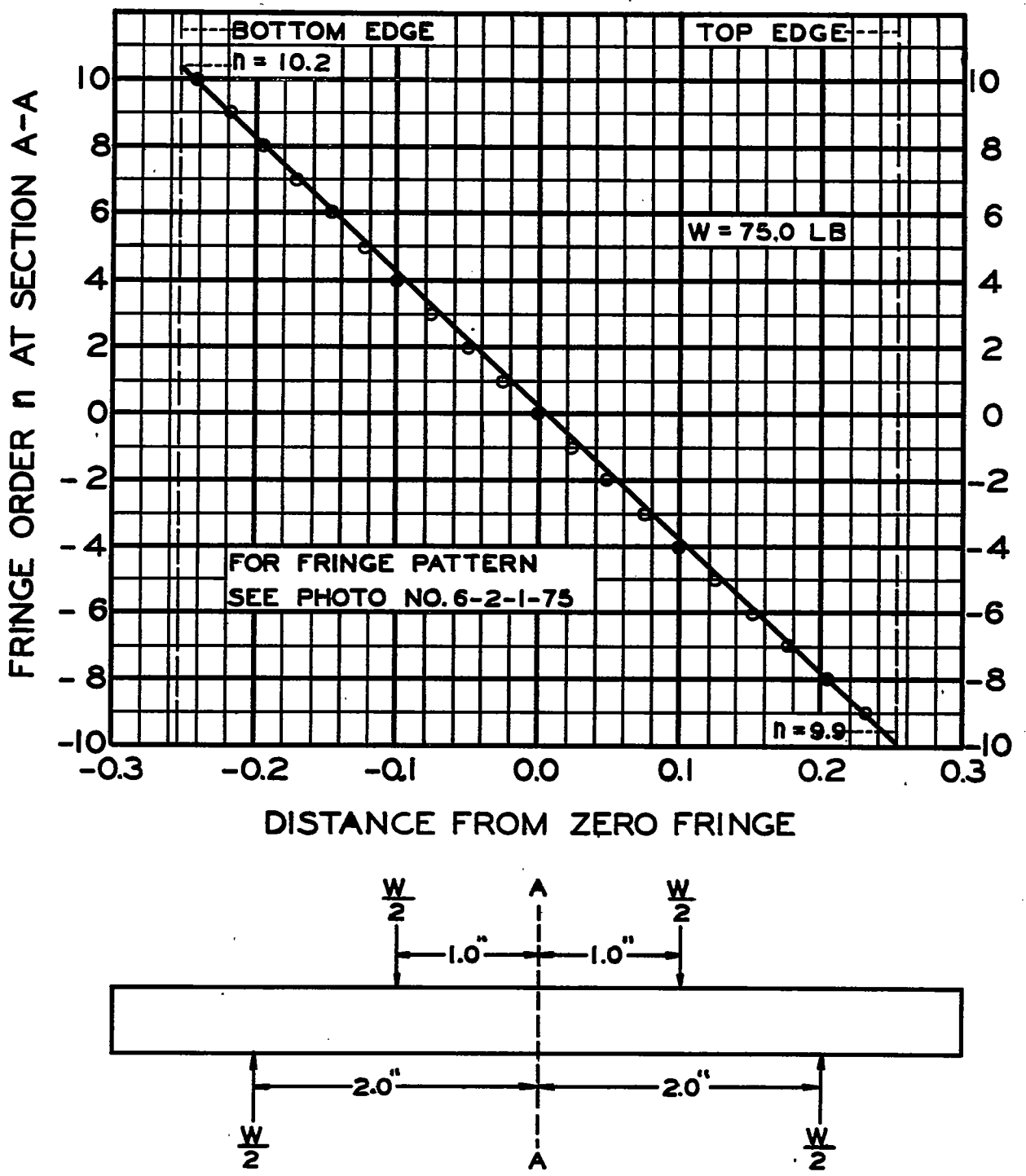

LOADING DIAGRAM FOR MODEL NO. 2

Figure 4.- Calibration test of model No. 2.

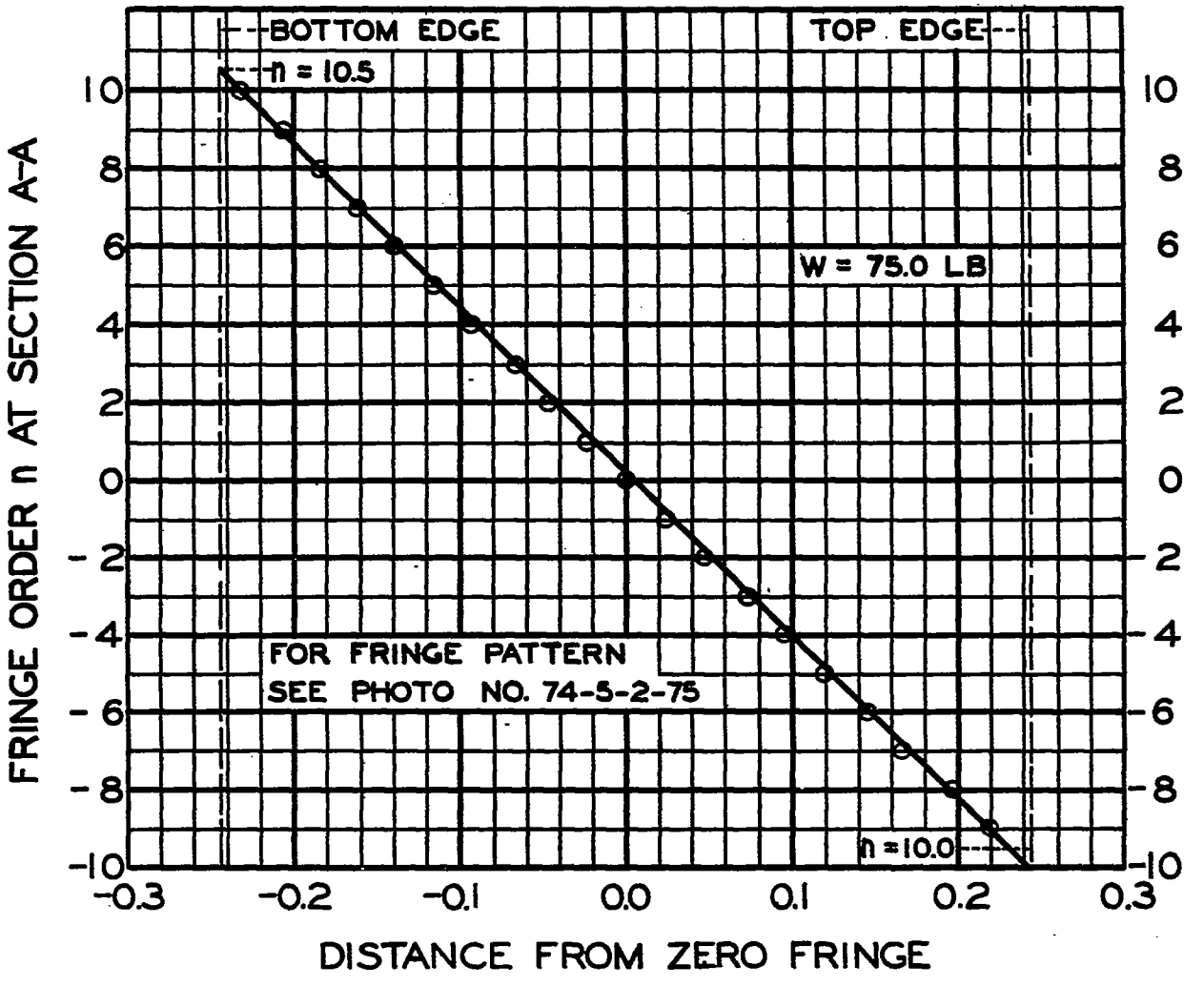

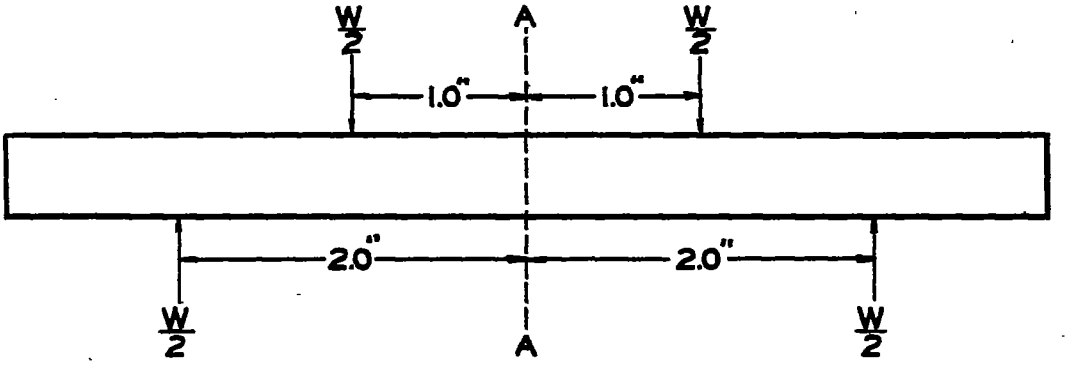

LOADING DIAGRAM FOR MODEL NO. 5

Figure 5.- Calibration test of model No. 5.

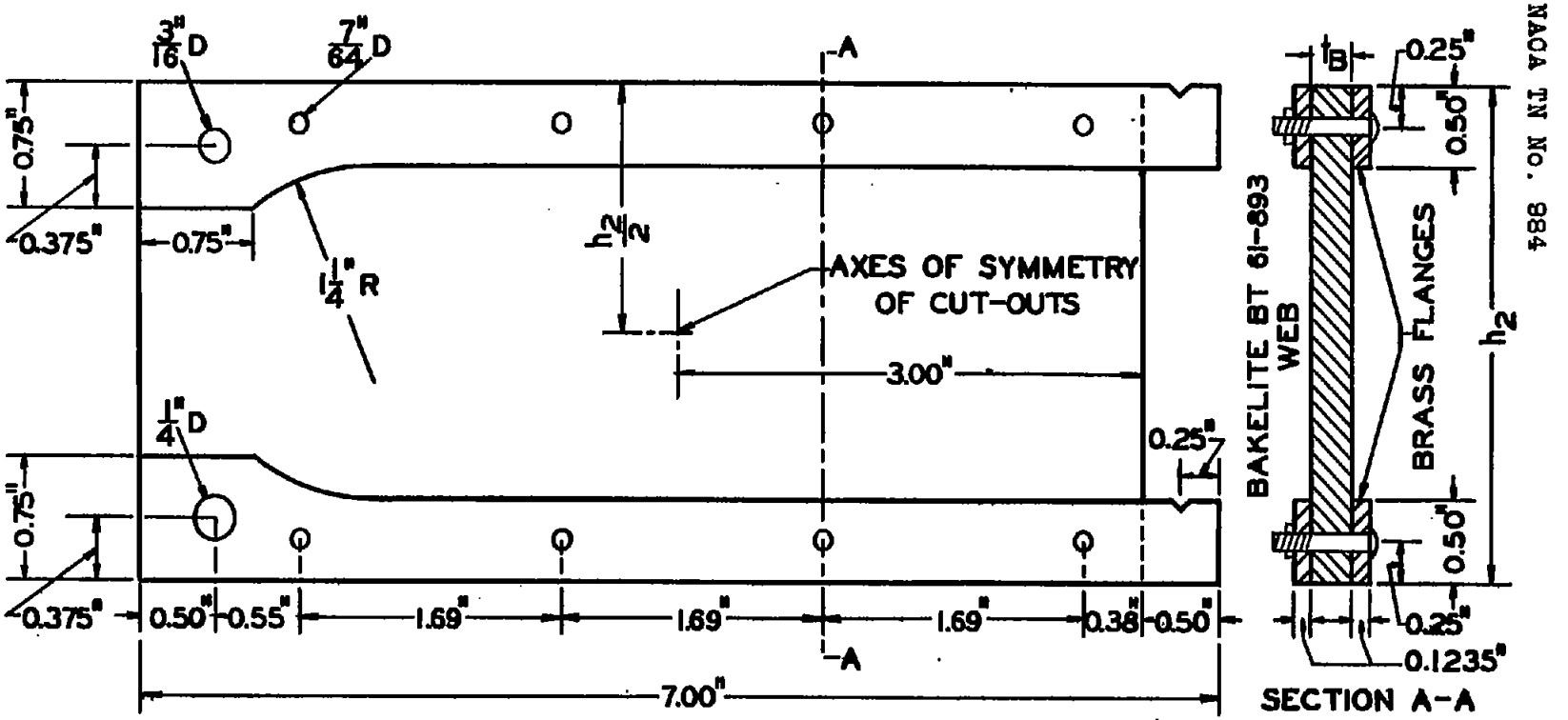

MODEL NO.	h_2	t_B
3	299	0.269
4	297	0.275
6	3.00	0.283
7	3.01	0.274
9	5.48	0.265

NOTE:- CUT-OUT DIMENSIONS SHOWN ON FIGURES AND TABLES.

SAME BRASS FLANGES USED ON ALL MODELS

Figure 6.- Models No. 3, 4, 6, 7 and 9.

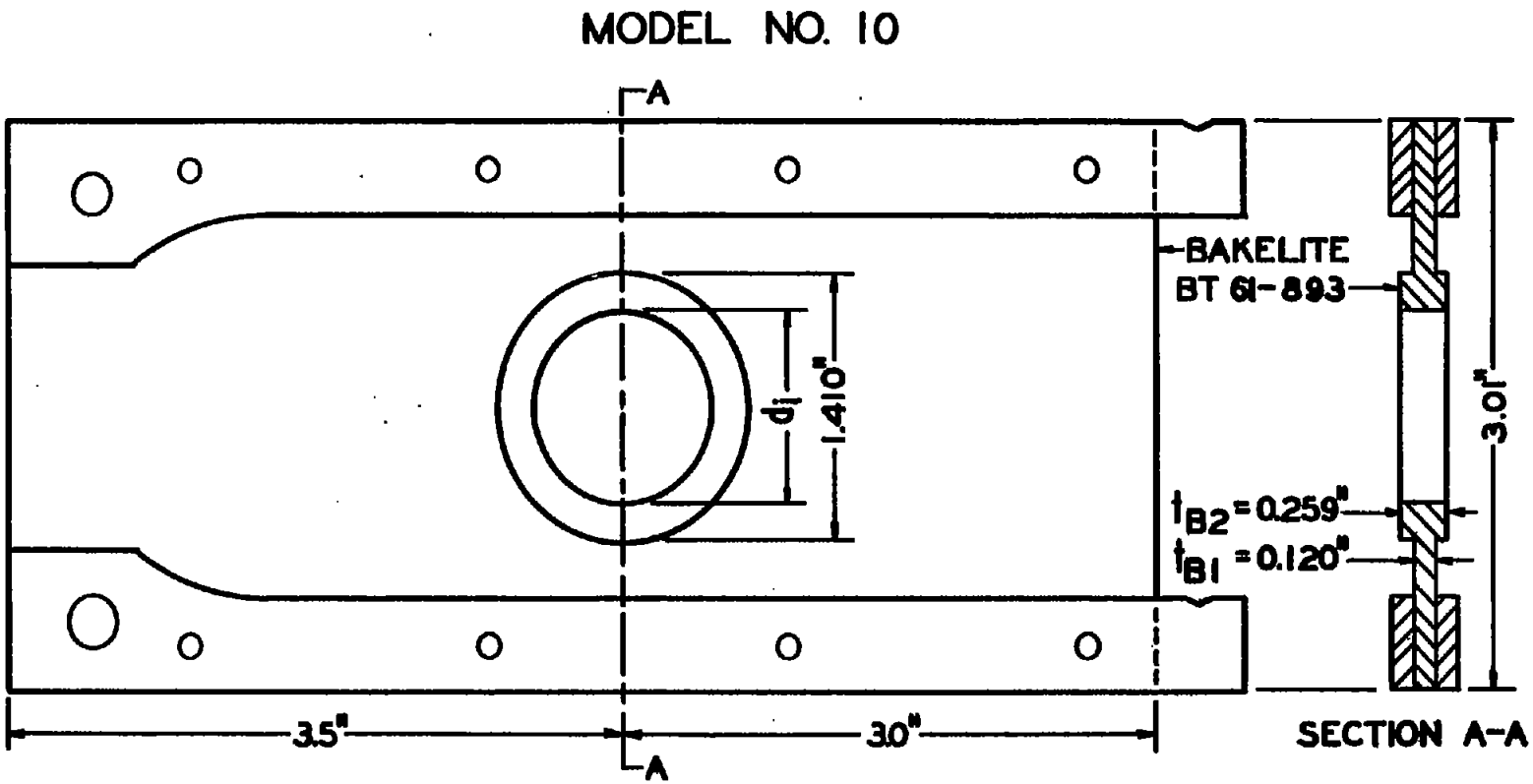

Figure 7.- Model No. 10.

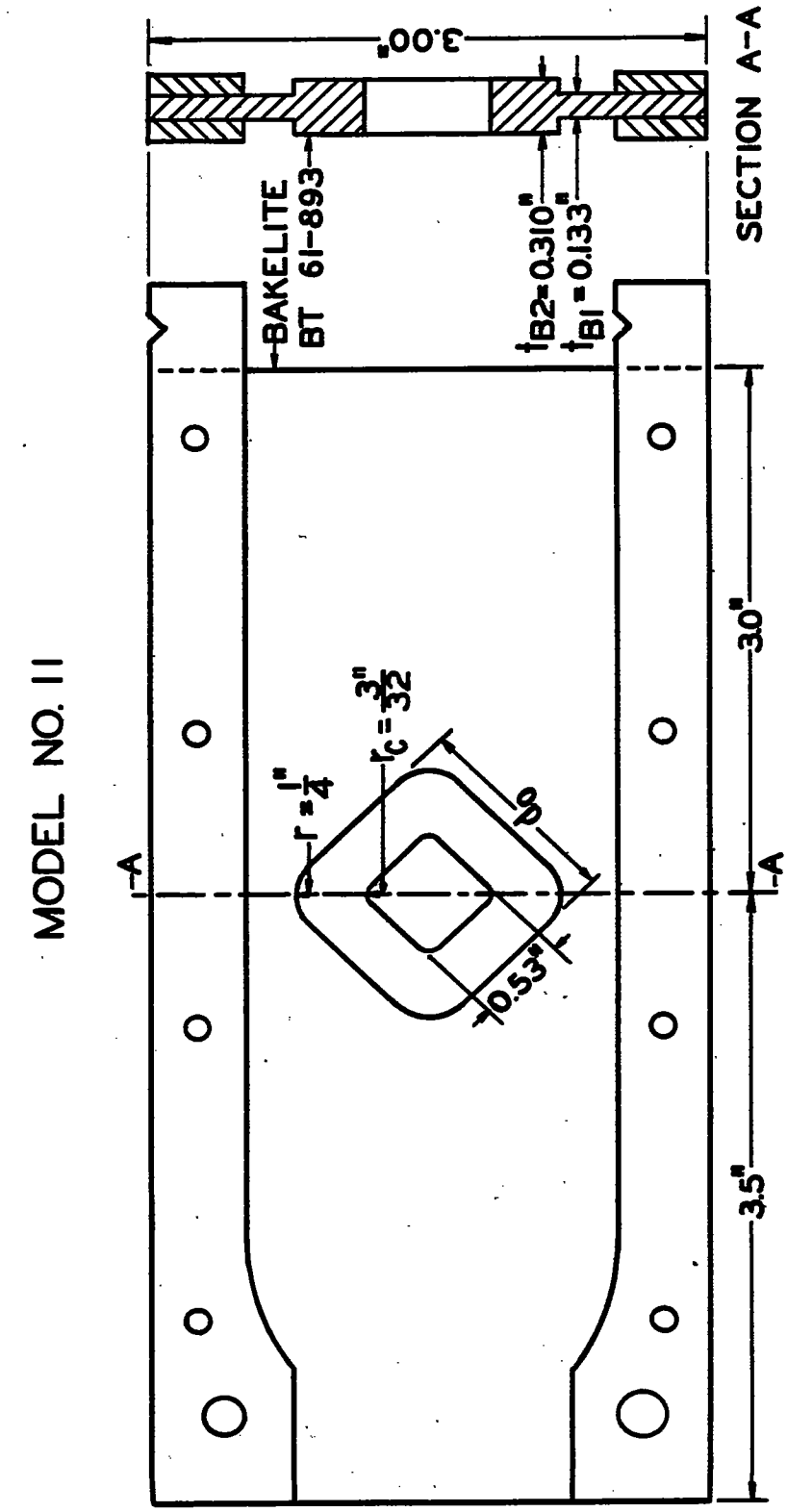

Figure 8.- Model No. 11.

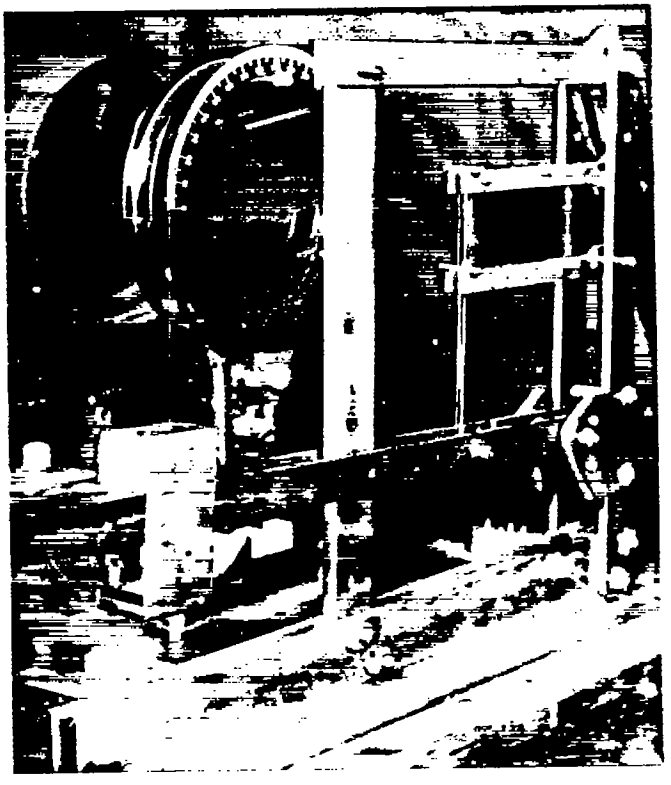

Figure 9.- Photograph of model set up for test.

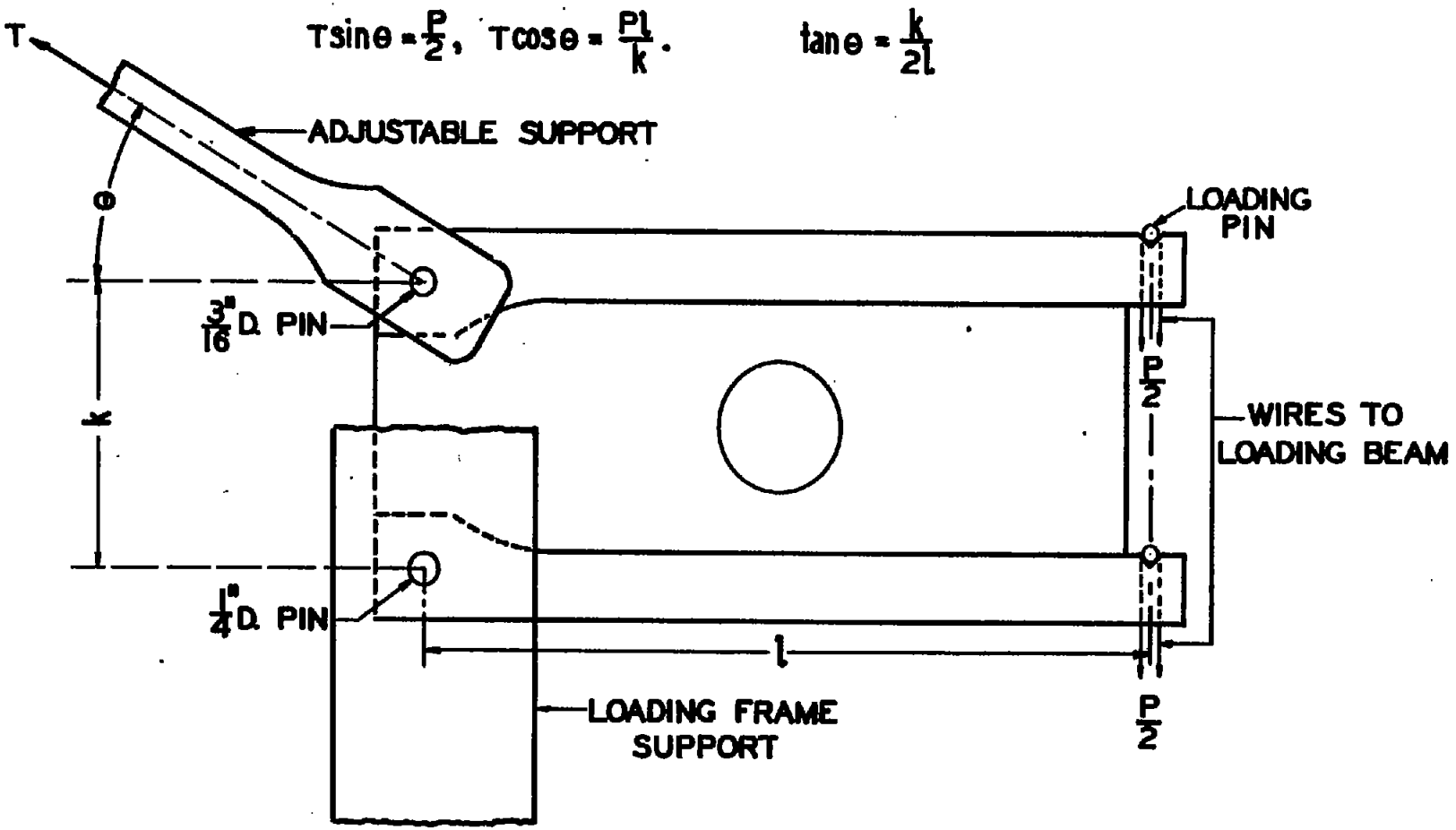

Figure 10.- Geometry of loading frame supports.

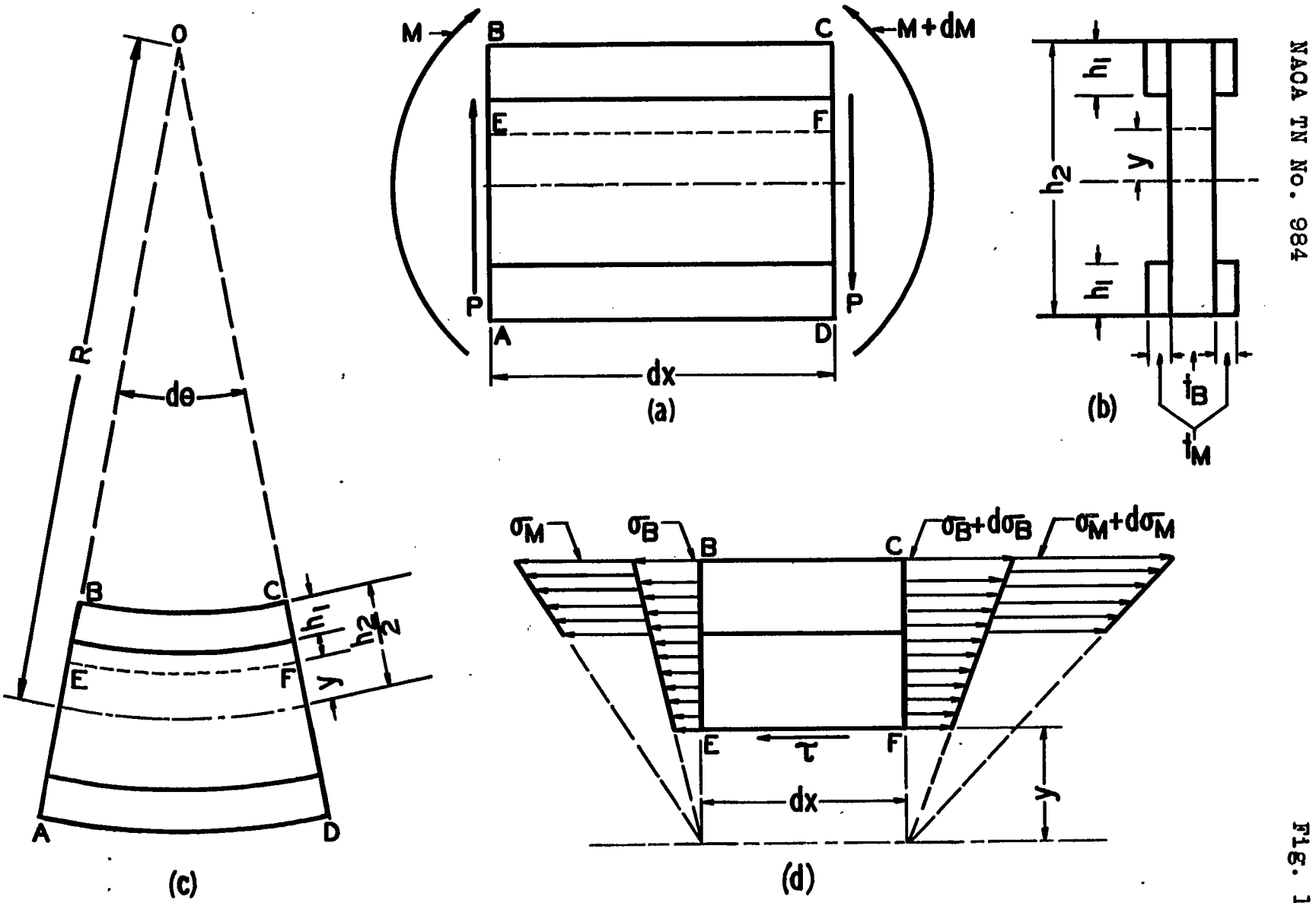

Figure 11.- Beam notation.

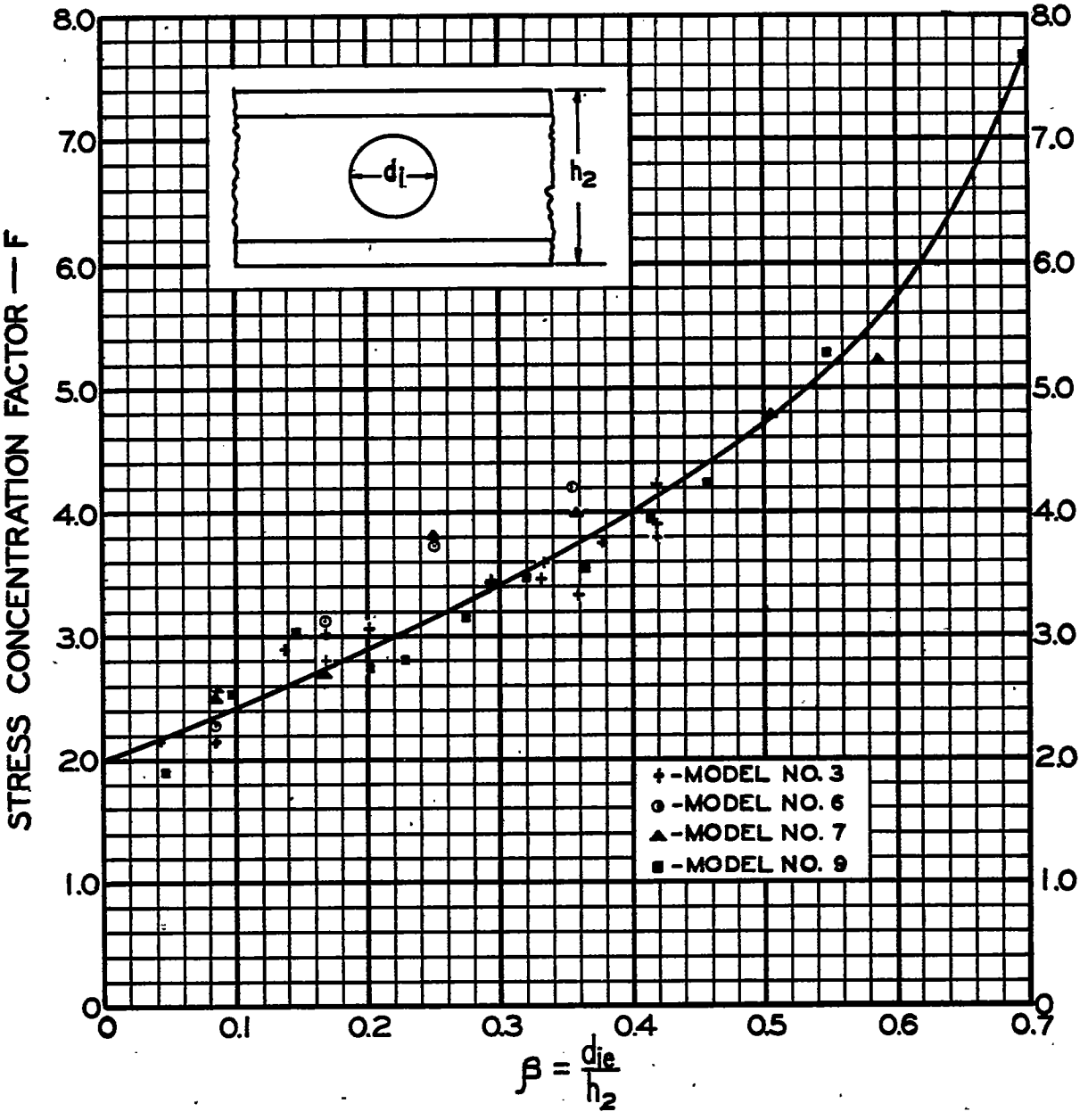

Figure 12.- Stress concentration factors for nonreinforced circular cut-outs.

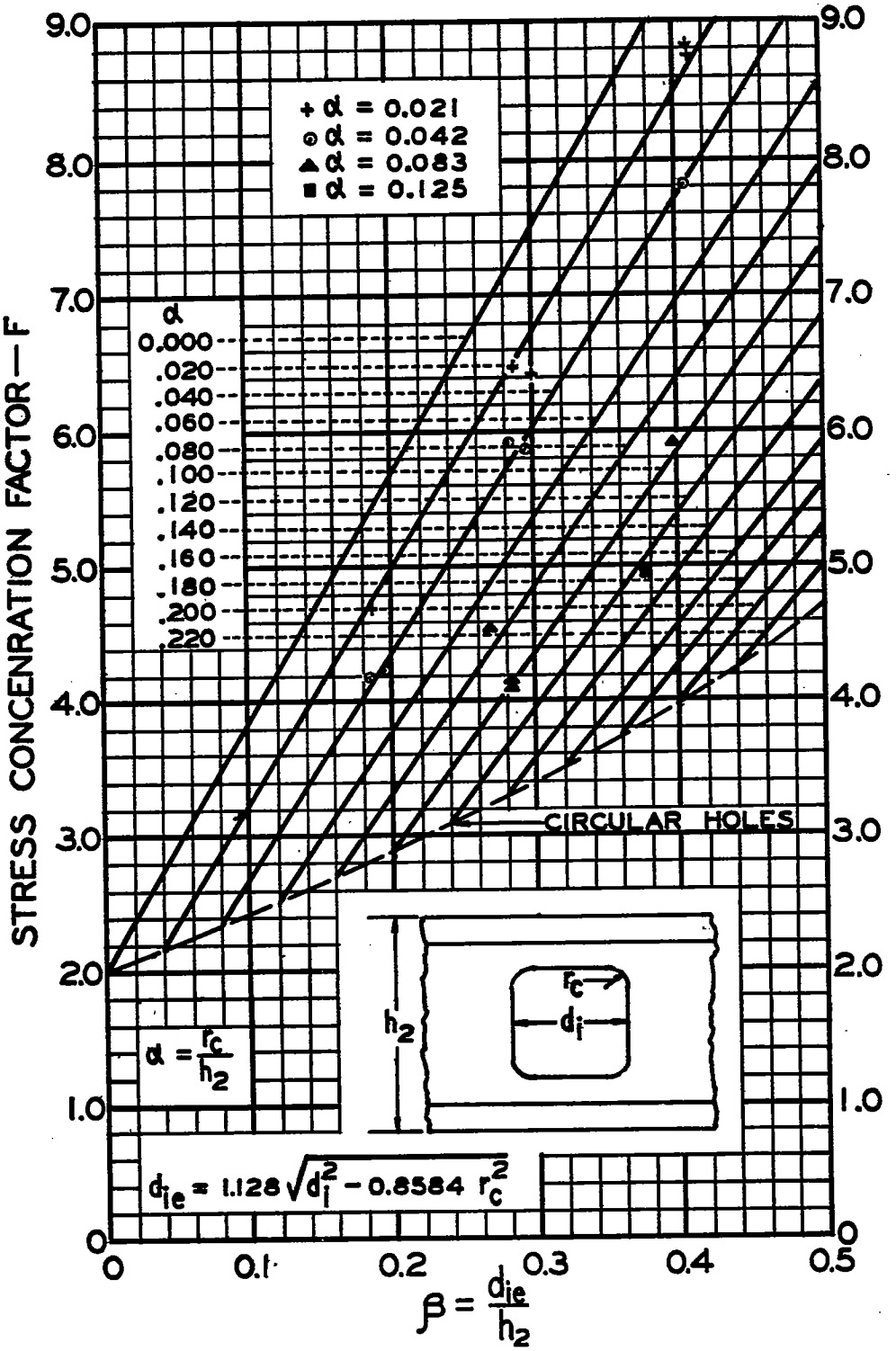

Figure 13.- Stress concentration factors for nonreinforced square cut-outs. Two sides of rectangles parallel to beam flanges.

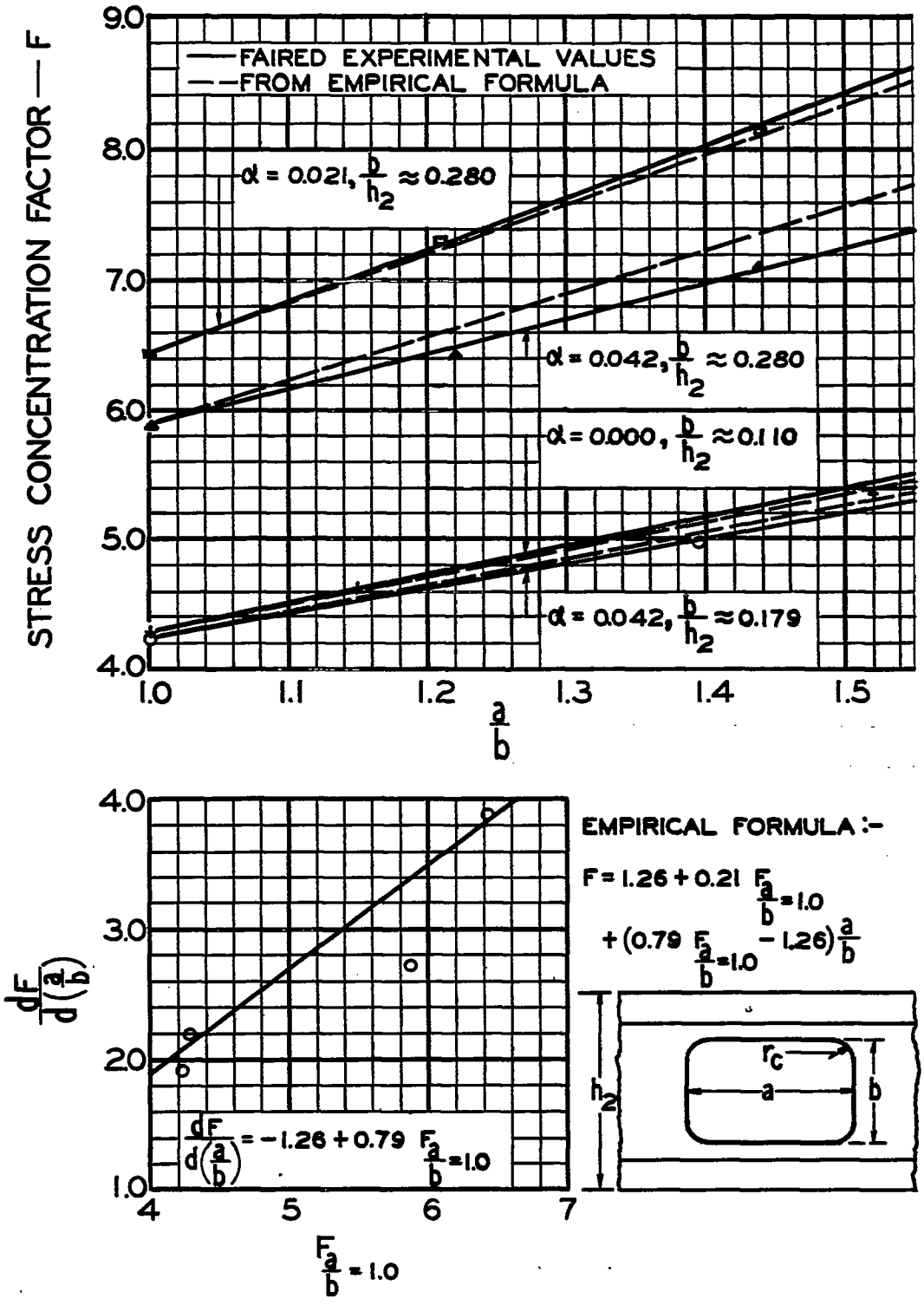

Figure 14.- Stress concentration factors for nonreinforced rectangular cut-outs. Two sides of rectangles parallel to beam flanges.

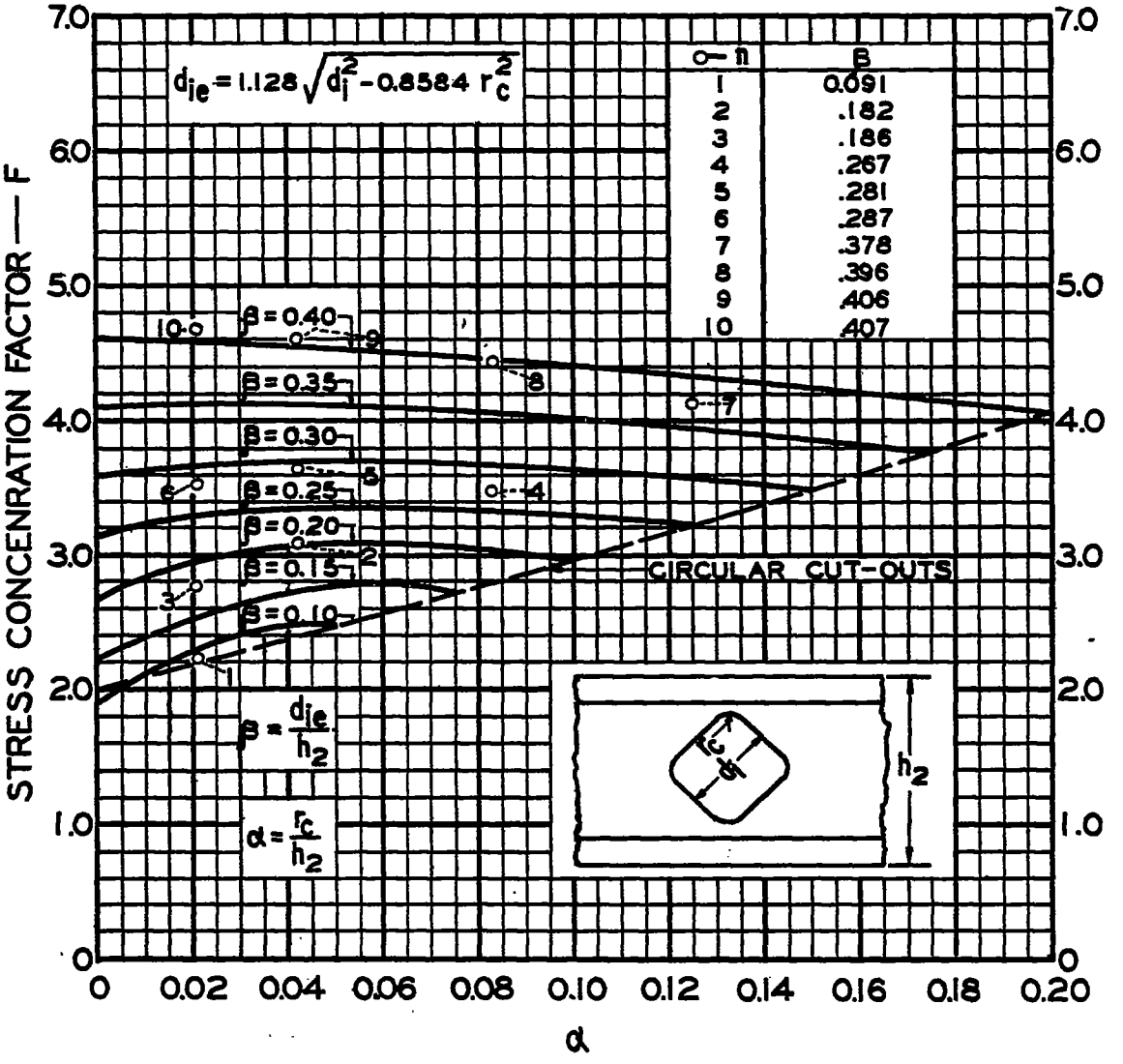

Figure 15.- Stress concentration factors for nonreinforced square cut-outs. Two sides of square 45° to beam flanges.

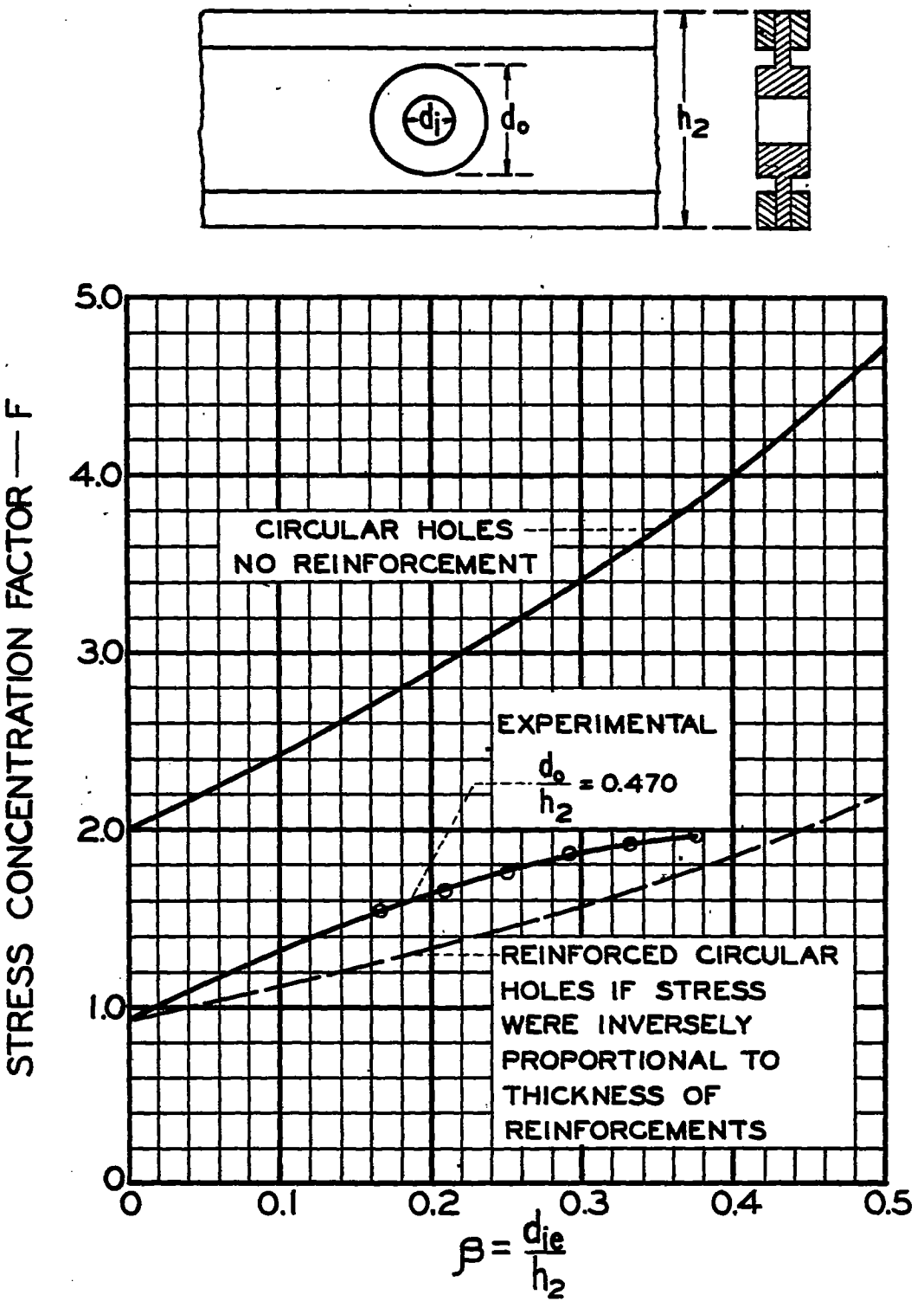

Figure 16.- Stress concentration factors for reinforced circular cut-outs.

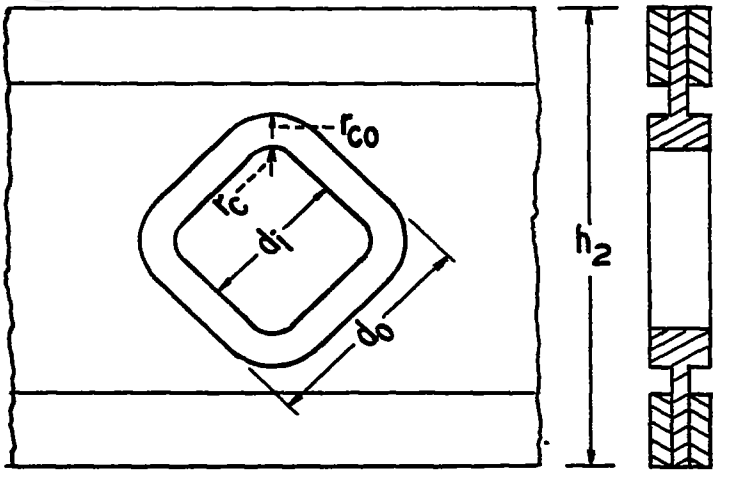

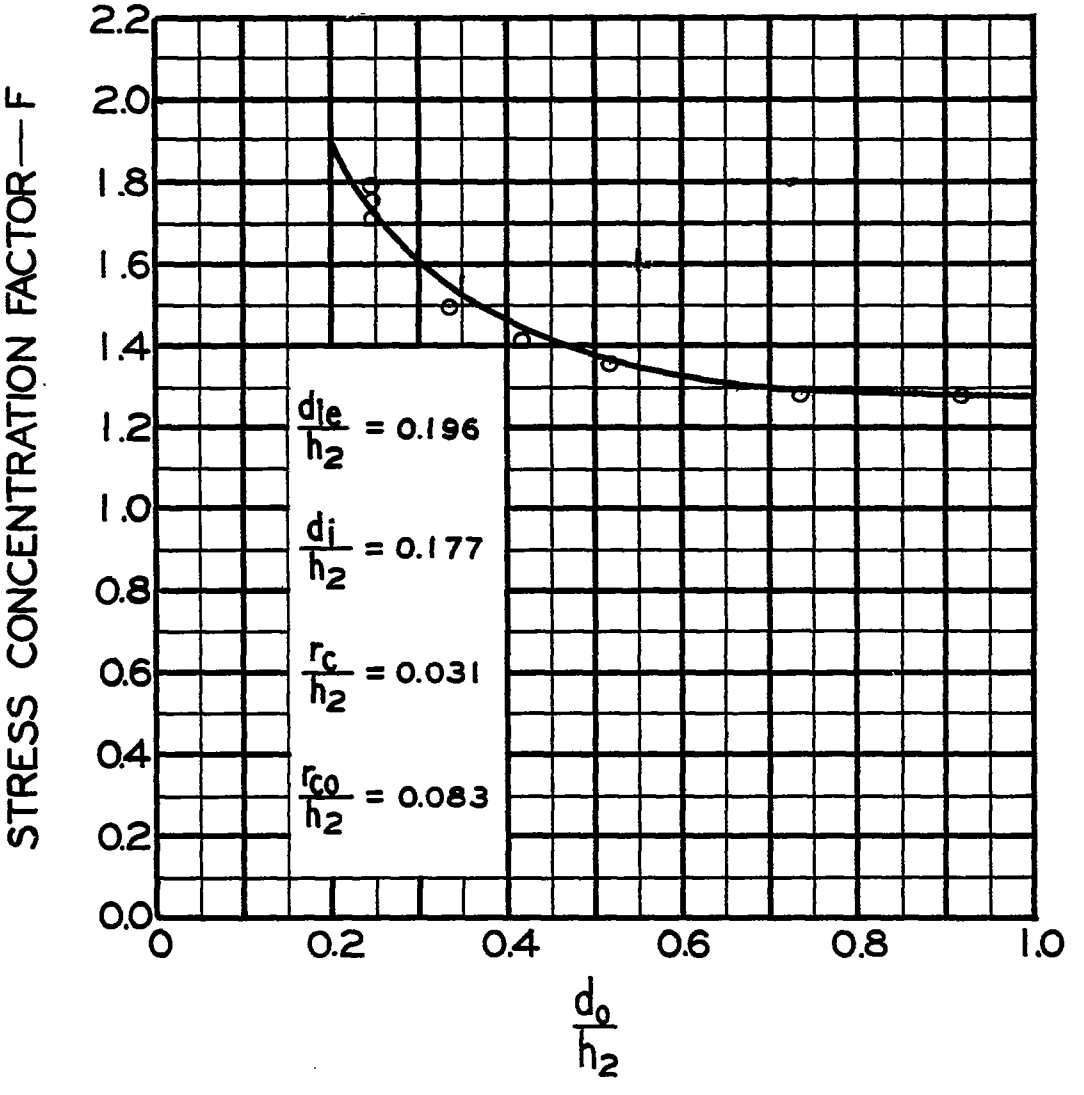

Figure 17.- Stress concentration factors for reinforced square cut-outs. Sides of squares 45° to flanges.

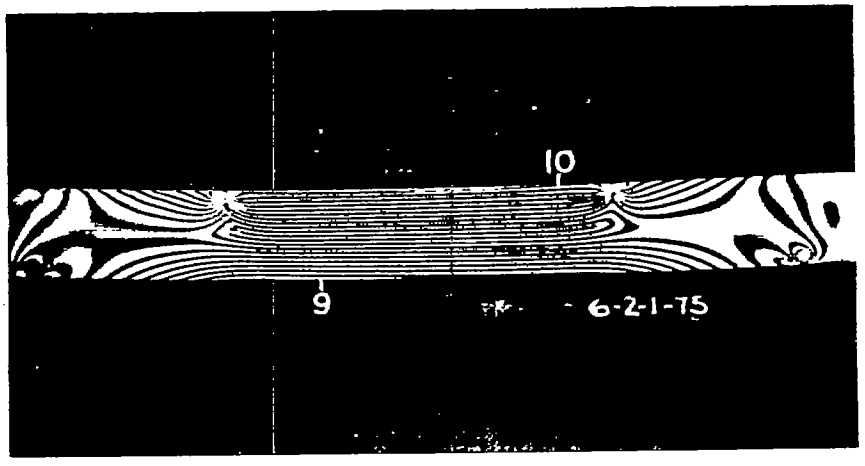

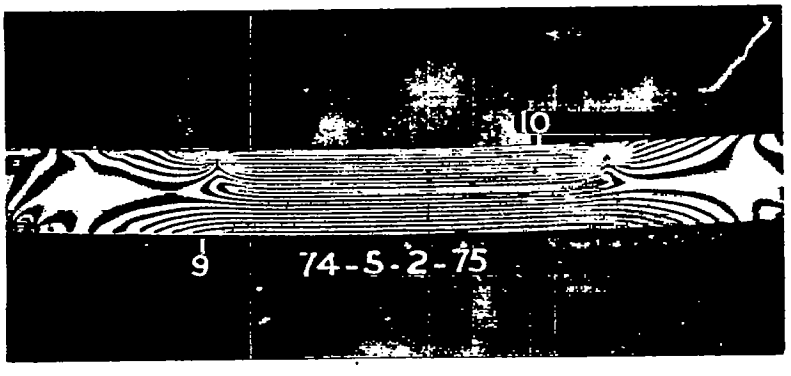

Figure 18.- Fringe patterns for bending tests.

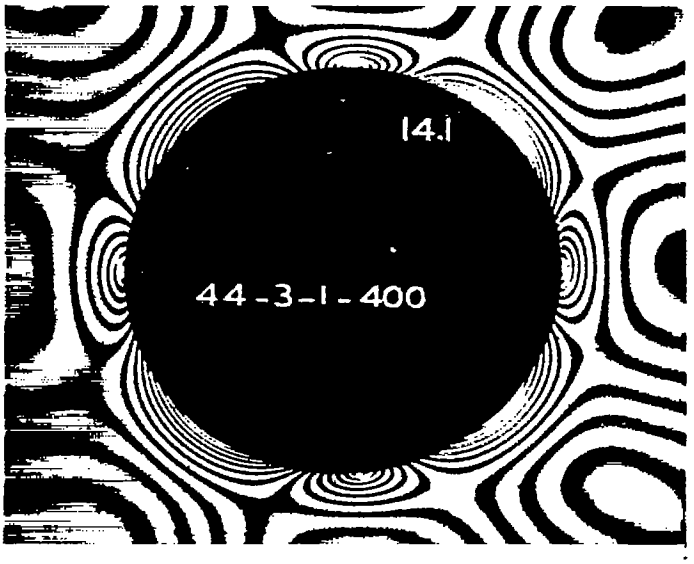

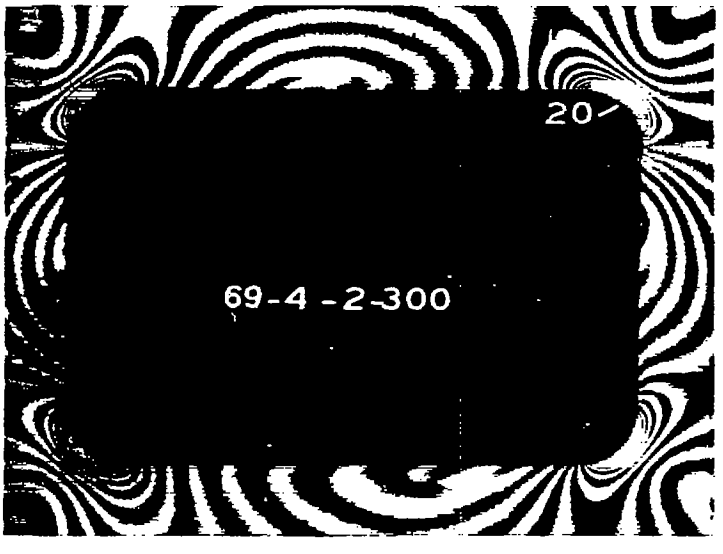

Figure 19a,b.- Typical fringe photographs.

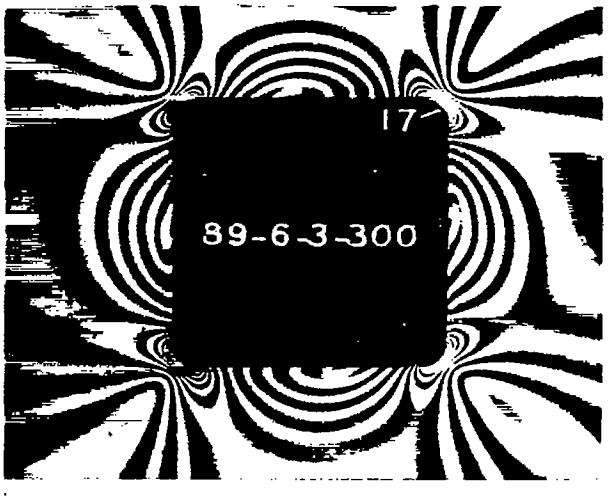

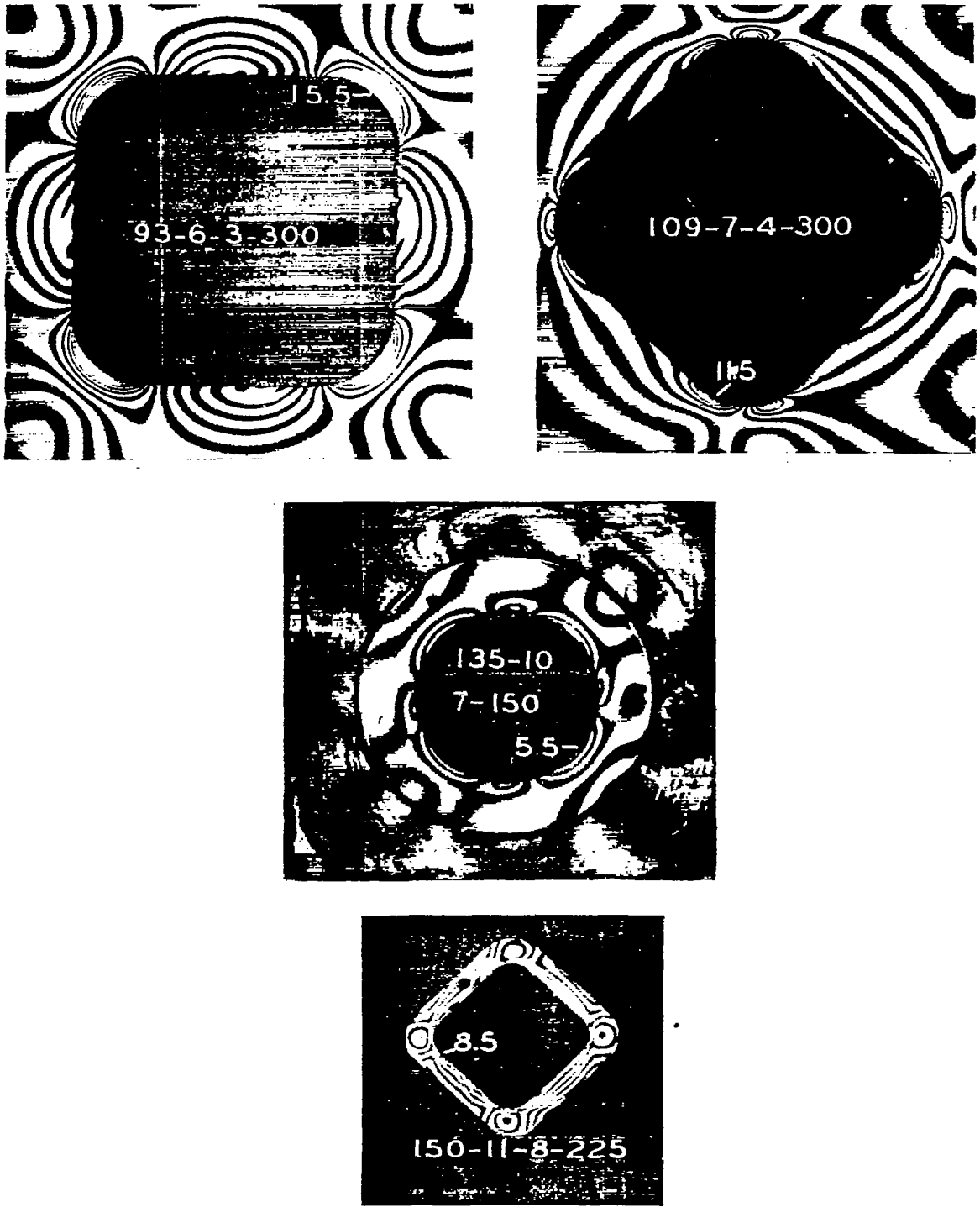

Figure 19.- Concluded.